[American Journal of Science, Vol. 299, Sept./Oct./Nov., 1999, P. 762–801]

BIOGEOCHEMICAL RESPONSES OF THE CARBON CYCLE TO NATURAL AND HUMAN PERTURBATIONS: PAST, PRESENT, AND FUTURE

LEAH MAY B. VER,* FRED T. MACKENZIE,* and ABRAHAM LERMAN**

ABSTRACT. In the past three centuries, human perturbations of the environment have affected the biogeochemical behavior of the global carbon cycle and that of the other three nutrient elements closely coupled to carbon: nitrogen, phosphorus, and sulfur. The partitioning of anthropogenic CO_2 among its various sinks in the past, for the present, and for projections into the near future is controlled by the interactions of these four elemental cycles within the major environmental domains of the land, atmosphere, coastal oceanic zone, and open ocean. We analyze the past, present, and future behavior of the global carbon cycle using the Terrestrial-Ocean-aTmosphere Ecosystem Model (TOTEM), a unique process-based model of the four global coupled biogeochemical cycles of carbon, nitrogen, phosphorus, and sulfur. We find that during the past 300 yrs, anthropogenic CO_2 was mainly stored in the atmosphere and in the open ocean. Human activities on land caused an enhanced loss of mass from the terrestrial organic matter reservoirs (phytomass and humus) mainly through deforestation and consequently increased humus remineralization, erosion, and transport to the coastal margins by rivers and runoff. Photosynthetic uptake by the terrestrial phytomass was enhanced owing to fertilization by increasing atmospheric CO_2 concentrations and supported by nutrients remineralized from organic matter. TOTEM results indicate that through most of the past 300 yrs, the loss of C from deforestation and other land-use activities was greater than the gain from the enhanced photosynthetic uptake. During the decade of the 1980s, the terrestrial organic reservoirs were in rough carbon balance. Organic and carbonate carbon accumulating in coastal marine sediments is a small but significant sink for anthropogenic CO_2. Increasing inputs of terrestrial organic matter and its subsequent oxidation in the coastal margin (increasing heterotrophy) were significant sources of CO_2 in coastal waters in the 20th century. However, the coastal ocean did not evolve into a greater net source of CO_2 to the atmosphere during this period because of the opposing pressure from rising atmospheric CO_2. Since pre-industrial time (since 1700), the net flux of CO_2 from the coastal waters has decreased by 40 percent, from 0.20 Gt C/yr to 0.12 Gt C/yr. TOTEM analyses of atmospheric CO_2 concentrations for the 21st century were based on the fossil-fuel emission projections of IPCC ("business as usual" scenario) and of the more restrictive UN 1997 Kyoto Protocol. By the mid-21st century, the projected atmospheric CO_2 concentrations range from about 550 ppmv (TOTEM, based on IPCC projected emissions) to 510 ppmv (IPCC projection) and to 460 ppmv (TOTEM, based on the Kyoto Protocol reduced emissions). The difference of about 40 ppmv between the IPCC and TOTEM estimates by the year 2050 reflects the different mechanisms within the C-N-P-S cycles on land that are built into our model. The effects of the reduced emissions prescribed by the Kyoto Protocol begin to show in the atmospheric CO_2 concentrations by the mid-21st century, when our model projects a rise to 460 (year 2050) and 490 ppmv (2075), relative to about 360 ppmv in 1995. However, these projected increases assume no major changes in the present biogeochemical feedback mechanisms within the system of the coupled C-N-P-S cycles, no global changes in the kind and distribution of ecosystems in response to the rising CO_2 and possibly temperature, and no changes in the mechanisms of CO_2 exchange between the atmosphere and the ocean, such as could be induced by changes in the intensity of oceanic thermohaline circulation.

* Department of Oceanography, SOEST, University of Hawaii, Honolulu, Hawaii 96822
** Department of Geological Sciences, Northwestern University, Evanston, Illinois 60208

I. INTRODUCTION

The recent history of the carbon cycle and atmospheric CO_2 is of interest both in a fundamental sense and because of the environmental issues related to the enhanced greenhouse effect and the potential of a future global warming of the planet Earth. For the past two decades, there has been uncertainty among scientists as to how anthropogenic carbon from fossil fuel burning and changes in land-use activities is partitioned between the sinks of atmosphere, ocean, and land. Atmospheric and oceanic observational data and model simulations confirm the importance of these sinks (Tans, Fung, and Takahashi, 1990; Tans, Berry, and Keeling, 1993; Keeling and Whorf, 1998). It has been known for a long time that the so-called "missing sink" in the global carbon cycle represents the excess of atmospheric emissions of carbon dioxide from fossil fuel burning and land-use activities over that accounted for by accumulation in the atmosphere and ocean. The magnitude of this missing sink, averaged for the period 1980 to 1989, was 1.8 Gt C/yr, amounting to about 55 percent of the annual accumulation in the atmosphere (3.3 Gt C/yr) or about the same as the annual accumulation in the oceans (2.0 Gt C/yr), out of the total of 7.1 Gt C/yr emitted from sources on land (Houghton and others, 1996). The large apparent imbalance in the global carbon budget has been addressed recently by postulating enhanced accumulation of organic carbon by the terrestrial biosphere (Tans, Fung, and Takahashi, 1990; Houghton and others, 1996; Bruno and Joos, 1997; Cao and Woodward, 1998a). Land plants might have been storing greater amounts of carbon through fertilization by (1) increasing atmospheric CO_2 concentrations, (2) warmer temperatures, and (3) increasing nitrogen and phosphorus inputs to terrestrial ecosystems from fertilizer application and atmospheric deposition of nitrogen-bearing chemical species (Houghton, Davidson, and Woodwell, 1998).

Although the postulated accumulation of carbon in the terrestrial phytomass and soils has yet to be detected in forests or other biomes on a global scale (Houghton, 1995), indirect evidences of an enhanced fertilization flux exist. For example, observations of the $^{13}C/^{12}C$ ratio in atmospheric CO_2 (Ciais, Tans, and Schimel, 1995; Ciais and others, 1995) and multi-year observations of changes in atmospheric O_2/N_2 ratios (Keeling and Shertz, 1992; Keeling, Piper, and Heimann, 1996) suggest an enhanced biotic uptake flux in the Northern Hemisphere ranging from 2.0 to 3.3 Gt C/yr for the period 1991 to 1994. Slightly lower fluxes for the preceding decade of the 1980s have been estimated by C. D. Keeling and others (1996). This terrestrial biospheric sink is likely to respond nonlinearly to environmental perturbations, and the understanding of its behavior in the future is critical to the predictions of future atmospheric CO_2 concentrations and hence the rate of potential warming of the planet (Woodwell and others, 1995).

In this paper we analyze the behavior of the carbon cycle during the past 300 yrs of human perturbations of the environment, focusing on the fate of anthropogenic CO_2, its distribution among the Earth's surface reservoirs, and projections for the 21st century using the Terrestrial-Ocean-aTmosphere Ecosystem Model (TOTEM) (fig. 1). Our model of the global carbon cycle emphasizes its important dependence on, and interactions with, the cycles of nitrogen (N), phosphorus (P), and sulfur (S). Although sulfur is recognized as an environmentally important element, its role in the control of the carbon cycle at the time scales of decades to centuries is not as clearly established at this time as the roles of the other two elements essential to life, N and P. Therefore this paper deals mainly with the coupled cycles of C-N-P, without sulfur, in the discussion of the changes in the global carbon cycle.

The biogeochemical cycles in the major domains of atmosphere, land, and ocean are often studied by means of models, and the modeling approaches often vary and commonly depend on the modelers' primary interest within a particular domain. It was clear to us that some of the present terrestrial-ecological or ocean-atmosphere models, for example, would not be compatible with the sparse data that exist for some of the

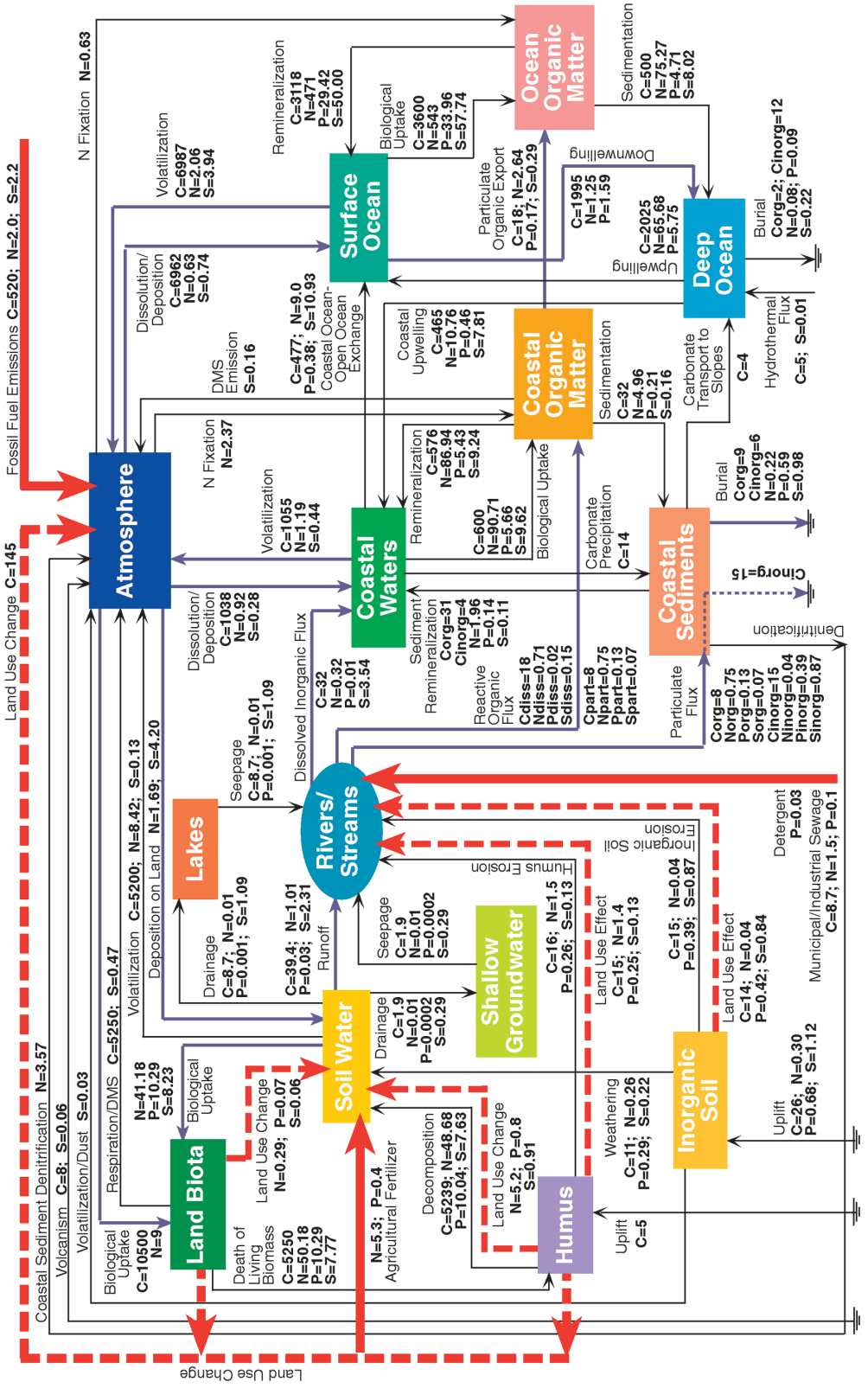
Atmosphere
Surface Ocean
Ocean Organic Matter
Deep Ocean
Coastal Organic Matter
Coastal Waters
Coastal Sediments
Rivers/ Streams
Lakes
Soil Water
Shallow Groundwater
Land Biota
Humus
Inorganic Soil
Fossil Fuel Emissions C=520; N=2.0; S=2.2
Land Use Change C=145
Coastal Sediment Denitrification N=3.57
Volcanism C=8; S=0.06
Volatilization/Dust S=0.03
N Fixation N=0.63
Volatilization C=6987 N=2.06 S=3.94
Remineralization C=3118 N=471 P=29.42 S=50.00
Biological Uptake C=3600 N=543 P=33.96 S=57.74
Sedimentation C=500 N=75.27 P=4.71 S=8.02
Particulate Organic Export C=18; N=2.64 P=0.17; S=0.29
Downwelling C=1995 N=1.25 P=1.59
Upwelling C=2025 N=65.68 P=5.75
Burial Corg=2; Cinorg=12 N=0.08; P=0.09 S=0.22
Dissolution/ Deposition C=6962 N=0.63 S=0.74
DMS Emission S=0.16
C=477; N=9.0 P=0.38; S=10.93 Coastal Ocean-Open Ocean Exchange
Coastal Upwelling C=465 N=10.76 P=0.46 S=7.81
Hydrothermal Flux C=5; S=0.01
Carbonate Transport to Slopes C=4
N Fixation N=2.37
Volatilization C=1055 N=1.19 S=0.44
Remineralization C=576 N=86.94 P=5.43 S=9.24
Sedimentation C=32 N=4.96 P=0.21 S=0.16
C=600 N=90.71 P=5.66 S=9.62
Biological Uptake
Carbonate Precipitation C=14
Burial Corg=9 Cinorg=6 N=0.22 P=0.59 S=0.98
Cinorg=15
Dissolution/ Deposition C=1038 N=0.92 S=0.28
Sediment Remineralization Corg=31 Cinorg=4 N=1.96 P=0.14 S=0.11
Reactive Organic Flux Cdiss=18 Ndiss=0.71 Pdiss=0.02 Sdiss=0.15
Particulate Flux Cpart=8 Npart=0.75 Ppart=0.13 Spart=0.07
Corg=8 Norg=0.75 Porg=0.13 Sorg=0.07 Cinorg=15 Ninorg=0.04 Pinorg=0.39 Sinorg=0.87
Denitrification
Seepage C=8.7; N=0.01 P=0.001; S=1.09
Dissolved Inorganic Flux C=32 N=0.32 P=0.01 S=3.54
Volatilization C=5200; N=8.42; S=0.13
Deposition on Land N=1.69; S=4.20
Volatilization C=5250; S=0.47
Respiration/DMS C=41.18 N=10.29 S=8.23
Biological Uptake C=10500 N=9
Drainage C=8.7; N=0.01 P=0.001; S=1.09
C=39.4; N=1.01 P=0.03; S=2.31 Runoff
Seepage C=1.9 N=0.01 P=0.0002 S=0.29
Drainage C=1.9 N=0.01 P=0.0002 S=0.29
Humus Erosion
Inorganic Soil Erosion
C=16; N=1.5 P=0.26; S=0.13
Land Use Effect C=15; N=1.4 P=0.25; S=0.13
C=15; N=0.04 P=0.39; S=0.87
Land Use Effect C=14; N=0.04 P=0.42; S=0.84
Detergent P=0.03
Municipal/Industrial Sewage C=8.7; N=1.5; P=0.1
Land Use Change N=0.29; P=0.07 S=0.06
Death of Living Biomass C=5250 N=50.18 P=10.29 S=7.77
N=5.3; P=0.4 Agricultural Fertilizer
Decomposition C=5239; N=48.68 P=10.04; S=7.63
Land Use Change N=5.2; P=0.8 S=0.91
Weathering C=11; N=0.26 P=0.29; S=0.22
Uplift C=5
Uplift C=26; N=0.30 P=0.68; S=1.12
Land Use Change

Figure 1

domains or the levels of accuracy that can be expected from simple, large-scale, aggregated global models. Accordingly, we adopted in our model those reservoirs and processes that would adequately represent the terrestrial as well as oceanic domains, with due regard to the methodological differences that characterize the terrestrial, atmospheric or oceanic models of other investigators. The general approach adopted in TOTEM was to treat the smallest number of reservoirs that was consistent with the ability of the model to detect representative, average changes in the biogeochemical behavior of C, N, and P over the period of progressively growing human perturbations of the environment of the past 300 yrs. Thus our study of the carbon cycle focuses on the decadal to century time scale of its past, present, and future.

II. MODEL STRUCTURE AND ANALYSIS

TOTEM is a process-driven model of the global biogeochemical cycles of the life-essential elements carbon, nitrogen, phosphorus, and sulfur. The model describes the biogeochemical and physical transport behavior of these elements in the four domains of the Earth's surface: land, atmosphere, coastal ocean, and open ocean (Mackenzie and others, 1993; Ver, Mackenzie, and Lerman, 1994; Mackenzie, Lerman, and Ver, 1998; Mackenzie, Ver, and Lerman, 1998; Ver, Mackenzie, and Lerman, 1999). As defined in the model, the global surface environment is comprised of thirteen reservoirs (fig. 1): the atmosphere; six terrestrial reservoirs (living biota, humus, inorganic soil, continental soilwater, shallow groundwater, and lakes); three coastal-zone reservoirs (organic matter, water, and sediments); and three open ocean reservoirs (organic matter, surface water, and deep water). The rivers are not defined as a reservoir because the residence time of water in rivers with respect to recharge by atmospheric precipitation is very short, about 20 days (Berner and Berner, 1996). The initial masses in the year 1700 of C, N, P, and S in the global reservoirs defined above are given in table 1A. In addition, other initial conditions (mass transfer fluxes and flux constants), flux equations, and kinetic parameters, are given in table 1B–C and app. A. Detailed calculations involving derivation of these equations and estimates are provided in Ver (1998).

An essential feature of the model is the coupling between the C-N-P-S cycles at every biologically mediated transfer process, such as photosynthesis, autorespiration, decay, and burial. This provision for the diverse, process-based biogeochemical interactions between the four element cycles in the four environmental domains distinguishes TOTEM from most other models. The coupled-cycles approach is critical to modeling the responses of biogeochemical systems to global change because an anthropogenic or natural source of one of these elements, such as fossil fuel burning or humus respiration, is often a source of all three other elements.

The coupling of the individual cycles is achieved in the model by the average C:N:S:P ratios associated with oceanic and terrestrial photosynthesis (Redfield ratios, Redfield, Ketchum, and Richards, 1963), autorespiration on land and in ocean waters, humus formation, and sedimentation of organic matter in the coastal zone and open

Fig. 1. Conceptual diagram of TOTEM (Terrestrial-Ocean-aTmosphere Ecosystem Model), an Earth system model of the C-N-P-S coupled biogeochemical cycles in four domains: land, atmosphere, coastal zone, and open ocean. Heavy red arrows: fluxes of the elements owing to perturbations from fossil fuel combustion, application of agricultural fertilizers, and municipal sewage and wastewater disposal. Heavy dashed red arrows: fluxes from the terrestrial organic and inorganic reservoirs affected by land-use activities. Medium-size blue arrows: natural fluxes that have been significantly modified by human activities. Thin black arrows: fluxes that have been less affected by the perturbations. Flux values shown for the blue and black arrows are at the initial conditions at an assumed steady state prior to 1700, whereas those for the red arrows are for 1995. Flux units are 10^{12} moles/yr of the element shown. (To recalculate fluxes into units of Gt/yr, multiply C flux by 0.012, N flux by 0.014, P flux by 0.031, and S flux by 0.032). Note that significant figures are retained to preserve material balance at steady state.

ocean. We make a simplifying assumption that these biologically mediated coupling processes are generic and apply over many different species and environments within the terrestrial or oceanic domains, and occur with the same global mean elemental ratios that do not change with time, on the decadal to century time scale. We recognize that the wide range of C:N:S:P values for terrestrial plants, phytoplankton, humus, and organic sediments found in the literature reflects the variations owing to differences in climatic conditions, ecosystem type, and the possibly transient conditions to which land and aquatic primary producers are adapted at any given time. For example, estimates for the Redfield C:N:S:P ratio for higher land plants vary from 510:4:0.8:1 (Delwiche and Likens, 1977) to 882:9:0.6:1 (Deevy, 1973) and 2057:17:3:1 (Likens, Bormann, and Johnson, 1981). In TOTEM, we adopt the C:N:S:P ratio for land plants of 510:4:0.8:1 (Delwiche and Likens, 1977), for oceanic plankton of 106:16:1.7:1 (Redfield, Ketchum, and Richards, 1963), for humus of 140:6.6:1.2:1 (Likens, Bormann, and Johnson, 1981), and the C:N:P ratio for organic matter in marine sediments of 250:20:1 (Ingall and Van Cappellen, 1990).

All the transfer processes between the model reservoirs are represented by linear or nonlinear equations describing reaction mechanisms and physical transport processes. Many details of the model have been reported elsewhere (Mackenzie and others, 1993; Ver, Mackenzie, and Lerman, 1994; Mackenzie, Lerman, and Ver, 1998; Mackenzie, Ver, and Lerman, 1998; Ver, 1998). In the following sections, we describe only those model relationships and parameters that are particularly relevant to terrestrial and oceanic processes that redistribute anthropogenic CO_2.

IIA. Transfer Processes And Flux Equations

IIA1. Terrestrial photosynthesis.–The exchange of CO_2 between the terrestrial biota and the atmosphere is one of the major fluxes in the global carbon cycle. How the terrestrial photosynthetic flux will respond to natural and anthropogenic perturbations, specifically to increasing atmospheric CO_2 concentrations, is uncertain. The close link between the atmospheric and terrestrial biotic reservoirs of C is confirmed by the temporal and spatial variations of atmospheric CO_2 concentration since the late 1950s that reflect the seasonal oscillations between net photosynthesis during the Northern Hemisphere summer and net respiration during the Northern Hemisphere winter. Evidence of a positive effect by rising atmospheric CO_2 on terrestrial photosynthetic rates is apparently revealed in the observed increase in amplitude of the high-latitude seasonal fluctuations in atmospheric CO_2 (Keeling, Chin, and Whorf, 1996; Myneni and others, 1997). Whether or not the terrestrial biota is, or will be in the future, a sink for anthropogenic CO_2 has significant implications to future climate change, terrestrial productivity, and other Earth system processes.

The photosynthetic production of terrestrial organic matter by plants is represented in TOTEM by the biochemical transformation of atmospheric C (C_{10}; designations used in TOTEM for the reservoirs, fluxes, and rate constants are given in table 1A-C) and inorganic nutrients N, P, and S from the continental soilwater reservoir (N_{Sw}, P_{Sw}, and S_{Sw}) to organic matter in the terrestrial phytomass reservoir (C_1, N_1, P_1, and S_1). The terrestrial gross photosynthetic uptake flux of C ($CF_{101} \equiv$ GPP, moles/yr) is given by the following relationship:

$$GPP(t) = kC_{101} \times C_1(t) \times K_{photo} \quad (1)$$

where kC_{101} in units of 1/yr is a rate constant, C_1 is the terrestrial biotic reservoir mass in units of 10^{12} moles, and K_{photo} is a dimensionless parameter that represents the depen-

TABLE 1

A. Global reservoir masses of total C, N, P, and S in units of moles, at the initial assumed steady state prior to the year 1700 (fig. 1).

Symbol	Reservoir	Carbon	Nitrogen	Phosphorus	Sulfur
1	Terrestrial phytomass	4.98×10^{16}	3.91×10^{14}	9.76×10^{13}	7.81×10^{13}
2	Reactive humus	2.05×10^{16}	9.76×10^{14}	1.47×10^{14}	1.71×10^{14}
3	Inorganic soil	5.98×10^{16}	1.23×10^{14}	1.15×10^{15}	8.63×10^{19}
4	Coastal water	6.0×10^{15}	6.0×10^{13}	4.50×10^{11}	8.46×10^{16}
5	Coastal organic matter	3.67×10^{14}	3.86×10^{14}	3.5×10^{12}	5.9×10^{12}
6	Coastal sediments	2.07×10^{17}	2.28×10^{15}	9.2×10^{15}	1.21×10^{16}
7	Ocean surface water	6.56×10^{16}	3.5×10^{13}	5.0×10^{13}	9.27×10^{17}
8	Ocean organic matter	3.82×10^{15}	2.13×10^{14}	3.61×10^{13}	6.13×10^{13}
9	Deep ocean water	2.90×10^{18}	5.11×10^{16}	4.53×10^{15}	3.80×10^{19}
	Dissolved inorganic	2.84×10^{18}	4.70×10^{16}	4.0×10^{15}	3.80×10^{19}
	Total organic	6.0×10^{16}	4.1×10^{15}	5.3×10^{14}	9.08×10^{14}
10	Atmosphere	4.90×10^{16}	2.8×10^{20}		9.5×10^{10}
Gw	Shallow groundwater	3.45×10^{15}	2.96×10^{12}	2.7×10^{11}	1.55×10^{18}
La	Lakes	1.04×10^{14}	1.0×10^{11}	8.0×10^{9}	1.25×10^{14}
R	Rivers	3.53×10^{12}	1.1×10^{11}	3.0×10^{10}	4.4×10^{11}
Sw	Soilwater	2.48×10^{14}	5.1×10^{12}	1.6×10^{11}	1.34×10^{12}

dence of photosynthetic carbon uptake on other environmental parameters, as defined below. The gross photosynthetic uptake rates of N, P, and S (NF_{Sw1}, PF_{Sw1}, and SF_{Sw1}, respectively) are calculated from GPP by applying the appropriate Redfield-type C:X ratio (where X = N, P, or S) for terrestrial phytomass uptake (see app. A).

The first two terms on the right hand side of eq (1) describe the photosynthetic uptake flux as a first-order kinetic process dependent on the mass of the terrestrial phytomass, conforming to the intuitive idea that biota grows and respires in proportion to its mass (Bacastow and Keeling, 1973). The rate constant kC_{101} is derived from the assumed steady-state values for the year 1700 of the carbon mass in terrestrial phytomass and the photosynthetic uptake flux (table 1C). The factor K_{photo} represents the coupling between the C, N, and P cycles through the dependence of GPP on atmospheric CO_2, N, and P concentrations in continental soilwater and temperature;

$$K_{photo} = f_{C10} \times f_{Nsw} \times f_{Psw} \times f_T \tag{2}$$

Each of the four terms on the right hand side of eq (2) represents a number of generalized ecological and physiological response relationships rather than empirical results from single literature sources. The f terms, defined below, vary with time, making K a time-dependent parameter.

Factor f_{C10} is the response function to changes in atmospheric CO_2, calculated using a Michaelis-Menten relationship (hyperbolic reaction kinetics);

$$f_{C10} = \frac{R_{max,C}}{CF_{101t=0}} \times \frac{C_{10}(t)}{k_C + C_{10}(t)} \tag{3}$$

TABLE 1

B. Global transfer fluxes of total C, N, P, and S at the initial assumed steady state prior to the year 1700 (fig. 1). Fluxes are in units of 10^{12} moles/yr, represented by XF_{ij}, where X = the element symbol C, N, P, or S, and the subscripts ij = the source reservoir i and sink reservoir j (table 1A). Note that significant figures are retained to preserve material balance at steady state.

Carbon		Nitrogen		Phosphorus		Sulfur	
Fluxes out of the Land Biota (Reservoir 1)							
CF_{12}	5250	NF_{12}	50.18	PF_{12}	10.294	SF_{12}	7.766
CF_{110}	5250					SF_{110}	0.469
Fluxes out of the Humus (Reservoir 2)							
CF_{2R}	16	NF_{2R}	1.50	PF_{2R}	0.258	SF_{2R}	0.133
CF_{2Sw}	5239	NF_{2Sw}	48.68	PF_{2Sw}	10.036	SF_{2Sw}	7.633
Fluxes out of the Inorganic Soil (Reservoir 3)							
						SF_{310}	0.031
CF_{3R}	15	NF_{3R}	0.04	PF_{3R}	0.387	SF_{3R}	0.872
CF_{3Sw}	11	NF_{3Sw}	0.26	PF_{3Sw}	0.290	SF_{3Sw}	0.221
Fluxes out of the Coastal Waters (Reservoir 4)							
CF_{45}	600	NF_{45}	90.71	PF_{45}	5.660	SF_{45}	9.623
CF_{46}	14						
CF_{47}	477	NF_{47}	9.00	PF_{47}	0.375	SF_{47}	10.929
CF_{410}	1055	NF_{410}	1.19			SF_{410}	0.435
Fluxes out of Coastal Organic Matter (Reservoir 5)							
CF_{54}	576	NF_{54}	86.94	PF_{54}	5.430	SF_{54}	9.238
CF_{56}	32	NF_{56}	4.96	PF_{56}	0.208	SF_{56}	0.157
CF_{58}	18	NF_{58}	2.64	PF_{58}	0.170	SF_{58}	0.289
						SF_{510}	0.156
Fluxes out of Coastal Sediments (Reservoir 6)							
$CF_{64\ org}$	31						
$CF_{64\ inorg}$	4	NF_{64}	1.96	PF_{64}	0.136	SF_{64}	0.113
CF_{69}	4						
		NF_{610}	3.57				
$CF_{6out\ inorg}$	21						
$CF_{6out\ org}$	9	NF_{6out}	0.22	PF_{6out}	0.588	SF_{6out}	0.982
Fluxes out of Ocean Surface Waters (Reservoir 7)							
CF_{78}	3600	NF_{78}	543	PF_{78}	33.96	SF_{78}	57.736
CF_{79}	1995	NF_{79}	1.25	PF_{79}	1.590		
CF_{710}	6987	NF_{710}	2.06			SF_{710}	3.939

Michaelis-Menten kinetic relationships are also used to describe the response functions of photosynthetic rate to available inorganic nutrient N and P in the continental soilwater reservoir;

$$f_{Nsw} = \frac{R_{max,N}}{NF_{Sw1t=0}} \times \frac{N_{Sw}(t)}{k_N + N_{Sw}(t)} \tag{4}$$

$$f_{Psw} = \frac{R_{max,P}}{PF_{Sw1t=0}} \times \frac{P_{Sw}(t)}{k_P + P_{Sw}(t)} \tag{5}$$

The Redfield ratio of uptake is assumed to be preserved in the Michaelis-Menten constants R_{max} and k. With these definitions of the parameters, the photosynthetic rate

TABLE 1B
(continued)

Carbon		Nitrogen		Phosphorus		Sulfur	
Fluxes out of Ocean Organic Matter (Reservoir 8)							
CF_{87}	3118	NF_{87}	471	PF_{87}	29.42	SF_{87}	50.006
CF_{89}	500	NF_{89}	75.27	PF_{89}	4.71	SF_{89}	8.019
Fluxes out of Deep Ocean Waters (Reservoir 9)							
CF_{94}	465	NF_{94}	10.76	PF_{94}	0.456	SF_{94}	7.814
CF_{97}	2025	NF_{97}	65.68	PF_{97}	5.755		
$CF_{9out\ inorg}$	12						
$CF_{9out\ org}$	2	NF_{9out}	0.08	PF_{9out}	0.089	SF_{9out}	0.218
Fluxes out of Atmosphere (Reservoir 10)							
CF_{101}	10500	NF_{101}	9				
CF_{104}	1038	NF_{104}	0.92			SF_{104}	0.281
		NF_{105}	2.37				
CF_{107}	6962	NF_{107}	0.63			SF_{107}	0.74
		NF_{108}	0.63				
		NF_{10Sw}	1.69			SF_{10Sw}	4.197
Flux out of Shallow Groundwater (Reservoir Gw)							
CF_{GwR}	1.9	NF_{GwR}	0.01	PF_{GwR}	0.0002	SF_{GwR}	0.288
Flux out of Lakes (Reservoir La)							
CF_{LaR}	8.7	NF_{LaR}	0.01	PF_{LaR}	0.001	SF_{LaR}	1.094
Fluxes out of Rivers (Reservoir R)							
CF_{R4}	32	NF_{R4}	0.32	PF_{R4}	0.013	SF_{R4}	3.541
$CF_{R5\ diss}$	18	$NF_{R5\ diss}$	0.71	$PF_{R5\ diss}$	0.019	$SF_{R5\ diss}$	0.150
$CF_{R5\ part}$	8	$NF_{R5\ part}$	0.75	$PF_{R5\ part}$	0.129	$SF_{R5\ part}$	0.067
$CF_{R6\ inorg}$	15	$NF_{R6\ inorg}$	0.04	$PF_{R6\ inorg}$	0.387	$SF_{R6\ inorg}$	0.872
$CF_{R6\ org}$	8	$NF_{R6\ org}$	0.75	$PF_{R6\ org}$	0.129	$SF_{R6\ org}$	0.067
Fluxes out of Continental Soilwater (Reservoir Sw)							
		NF_{Sw1}	41.18	PF_{Sw1}	10.294	SF_{Sw1}	8.235
CF_{Sw10}	5200	NF_{Sw10}	8.42			SF_{Sw10}	0.125
CF_{SwGw}	1.9	NF_{SwGw}	0.01	PF_{SwGw}	0.0002	SF_{SwGw}	0.288
CF_{SwLa}	8.7	NF_{SwLa}	0.01	PF_{SwLa}	0.001	SF_{SwLa}	1.094
CF_{SwR}	39.4	NF_{SwR}	1.01	PF_{SwR}	0.031	SF_{SwR}	2.309
External Input Fluxes							
CF_{out2}	5						
CF_{out3}	26	NF_{out3}	0.30	PF_{out3}	0.677	SF_{out3}	1.124
CF_{out10}	8					SF_{out10}	0.063
CF_{hydro}	5					SF_{hydro}	0.013

tends to a constant value, R_{max}/(Flux at t = 0), as the nutrient concentration increases indefinitely, and it decreases with declining nutrient concentrations (in the preceding equations, reservoir masses and fluxes are in units of 10^{12} mol and 10^{12} mol/yr, respectively, table 1A-B and app. A).

The functional dependence of GPP on temperature generally varies considerably among plant taxa, soils, and local climatic conditions. Drawing from the observations of a positive effect of elevated temperature on photosynthesis (Larcher, 1983; Harvey, 1989; Lashof, 1989; Kohlmaier, Janecek, and Kindermann, 1990), the term f_T is defined as;

$$f_T = Q_{10}^{(T-T_{1700})/10} \tag{6}$$

TABLE 1

C. Flux constants adopted in TOTEM at the initial condition of an assumed steady state prior to 1700 (fig. 1). Flux constants are in units of 1/yr and are represented by kX_{ij} (where X = C, N, P, or S) and the subscripts ij denote the source reservoir i and sink reservoir j (see table 1A).

Carbon	Nitrogen	Phosphorus	Sulfur
$kC_{12} = 5250/(4.98 \times 10^4)$	$kN_{12} = 50.18/391$	$kP_{12} = 10.294/97.65$	$kS_{12} = 7.766/78.1$
$kC_{110} = 5250/(4.98 \times 10^4)$			$kS_{110} = 0.469/78.1$
$kC_{2Sw} = 5239/(2.05 \times 10^4)$	$kN_{2Sw} = 48.68/976$	$kP_{2Sw} = 10.036/147$	$kS_{2Sw} = 7.633/170.5$
			$kS_{310} = 0.031/(8.63 \times 10^7)$
$kC_{3Sw} = 11/(5.98 \times 10^4)$	$kN_{3Sw} = 0.26/123$	$kP_{3Sw} = 0.29/(1.15 \times 10^3)$	$kS_{3Sw} = 0.221/(8.63 \times 10^7)$
$kC_{46} = 14/(6.0 \times 10^3)$			
$kC_{47} = 477/(6.0 \times 10^3)$	$kN_{47} = 9.00/60$	$kP_{47} = 0.375/0.45$	$kS_{47} = 10.929/(8.46 \times 10^4)$
	$kN_{410} = 1.19/60$		$kS_{410} = 0.435/(8.46 \times 10^4)$
$kC_{54} = 576/367$	$kN_{54} = 86.94/386$	$kP_{54} = 5.43/3.5$	$kS_{54} = 9.238/5.9$
$kC_{56} = 32/367$	$kN_{56} = 4.96/386$	$kP_{56} = 0.2080/3.5$	$kS_{56} = 0.1565/5.9$
$kC_{58} = 18/367$	$kN_{58} = 2.64/386$	$kP_{58} = 0.17/3.5$	$kS_{58} = 0.289/5.9$
			$kS_{510} = 0.156/5.9$
$kC_{64\ org} = 31/(2.07 \times 10^5)$	$kN_{64} = 1.96/(2.28 \times 10^3)$	$kP_{64} = 0.136/(9.2 \times 10^3)$	$kS_{64} = 0.113/(1.21 \times 10^4)$
$kC_{64\ inorg} = 4/(2.07 \times 10^5)$			
$kC_{69} = 4/(2.07 \times 10^5)$			
	$kN_{610} = 3.57/(2.28 \times 10^3)$		
$kC_{6out\ inorg} = 21/(2.07 \times 10^5)$			
	$kN_{79} = 1.25/35$	$kP_{79} = 1.59/50$	
	$kN_{710} = 2.06/35$		$kS_{710} = 3.939/(9.27 \times 10^5)$
$kC_{87} = 3118/(3.82 \times 10^3)$	$kN_{87} = 471/213$	$kP_{87} = 29.42/36.1$	$kS_{87} = 50.006/61.3$
$kC_{89} = 500/(3.82 \times 10^3)$	$kN_{89} = 75.27/213$	$kP_{89} = 4.71/36.1$	$kS_{89} = 8.019/61.3$
$kC_{94} = 465/(2.90 \times 10^6)$	$kN_{94} = 10.76/(5.11 \times 10^4)$	$kP_{94} = 0.456/(4.53 \times 10^3)$	$kS_{94} = 7.814/(3.8 \times 10^7)$
$kC_{9out\ inorg} = 12/(2.90 \times 10^6)$			
	$kN_{97} = 65.68/(5.11 \times 10^4)$	$kP_{97} = 5.755/(4.53 \times 10^3)$	
$kC_{101} = 10500/(4.98 \times 10^4)$			
	$kN_{104} = 0.92/(2.80 \times 10^8)$		$kS_{104} = 0.281/5.218$
	$kN_{107} = 0.63/(2.80 \times 10^8)$		$kS_{107} = 0.74/5.218$
	$kN_{10Sw} = 1.69/(2.80 \times 10^8)$		$kS_{10Sw} = 4.197/5.218$
$kC_{GwR} = 1.9/(3.45 \times 10^3)$	$kN_{GwR} = 0.01/2.96$	$kP_{GwR} = 0.0002/0.27$	$kS_{GwR} = 0.288/(1.55 \times 10^6)$
$kC_{LaR} = 8.7/104$	$kN_{LaR} = 0.01/0.10$	$kP_{LaR} = 0.001/0.008$	$kS_{LaR} = 1.094/125$
$kC_{R4} = 32/3.53$	$kN_{R4} = 0.32/0.11$	$kP_{R4} = 0.013/0.03$	$kS_{R4} = 3.541/0.44$
$kC_{R5\ diss} = 18/3.53$	$kN_{R5\ diss} = 0.71/0.11$	$kP_{R5\ diss} = 0.019/0.03$	$kS_{R5\ diss} = 0.15/0.44$
$kC_{R5\ part} = 8/3.53$	$kN_{R5\ part} = 0.75/0.11$	$kP_{R5\ part} = 0.129/0.03$	$kS_{R5\ part} = 0.0665/0.44$
$kC_{R6\ org} = 8/3.53$	$kN_{R6\ org} = 0.75/0.11$	$kP_{R6\ org} = 0.129/0.03$	$kS_{R6\ org} = 0.0665/0.44$
$kC_{R6\ inorg} = 15/3.53$	$kN_{R6\ inorg} = 0.04/0.11$	$kP_{R6\ inorg} = 0.387/0.03$	$kS_{R6\ inorg} = 0.872/0.44$
$kC_{Sw10} = 5200/248$	$kN_{Sw10} = 8.42/5.1$		$kS_{Sw10} = 0.125/1.34$
$kC_{SwGw} = 1.9/248$	$kN_{SwGw} = 0.01/5.1$	$kP_{SwGw} = 0.0002/0.16$	$kS_{SwGw} = 0.288/1.34$
$kC_{SwLa} = 8.7/248$	$kN_{SwLa} = 0.01/5.1$	$kP_{SwLa} = 0.001/0.16$	$kS_{SwLa} = 1.094/1.34$
$kC_{SwR} = 39.4/248$	$kN_{SwR} = 1.01/5.1$	$kP_{SwR} = 0.0308/0.16$	$kS_{SwR} = 2.309/1.34$

The Q_{10} function, commonly used in plant ecology and physiology, is the factor by which the rate of photosynthesis increases with a 10°C increase in temperature. T and T_{1700} are the global temperatures at times t and in the year 1700, in units of °C. Although it is recognized that there are data, however sparse, to support values of Q_{10} other than 2.0, the value of 2.0 is adopted as a working approximation in TOTEM (Ver, Mackenzie, and Lerman, 1994; Ver, 1998). Because the focus of interest with respect to changing temperature is the magnitude of change from the initial, steady-state condition, the temperature difference, $\Delta T = T - T_{1700}$, determines the change in the rate of photosynthesis. For a temperature rise of $\Delta T = 1$°C, the calculated factor is $f_T = 1.07$, corresponding to a 7 percent increase in the rate.

The function K_{photo} in eq (1) describes the response of gross primary production to changes in atmospheric CO_2 concentration, concentrations of the nutrients N and P in soilwater, and global mean temperature. As such, K is analogous to the "biotic growth factor," β, used by other investigators to describe the response of carbon uptake by the phytomass to changing CO_2 concentrations. At the initial conditions of the C-N-P-S

global system in the year 1700, the function K_{photo} is unity; subsequently, its value changes fractionally with the changing mass of C in the atmosphere, masses of N and P in soilwater, and global temperature. Keeling (1973a) first introduced a factor β, defined as the "degree of CO_2 fertilization," to express a logarithmic dependence in productivity on an increase in atmospheric CO_2. Since then, other mathematical formulations, varying from logarithmic relationships to the Michaelis-Menten formulation such as that used in this paper, have been proposed (see reviews and summaries by Bacastow and Keeling, 1973; Friedlingstein and others, 1995; and Wullschleger, Post, and King, 1995). A common feature of such formulations is the non-linear response of the rates of primary production to changes in atmospheric CO_2 concentration.

Generally, the studies that include β in global carbon models indicate that terrestrial ecosystems can sequester large amounts of carbon through a CO_2 fertilization effect on photosynthesis, and that this process might indeed function as a negative feedback to future increases in global atmospheric CO_2 (Goudriaan and Ketner, 1984; Kohlmaier and others, 1987; Raich and others, 1991; Sellers, Los, and Randall, 1996). In most carbon cycle models, the biotic growth factors used to balance the global carbon budget range in value from 0.2 to 0.5. A relatively high β value of 0.5 was used by Goudriaan and Ketner (1984; Goudriaan, 1989) to reproduce the measured atmospheric CO_2 trend over the period from 1958 to 1980. Bacastow and Keeling (1973) required a β value in the range of 0.4 to 0.5 to reproduce the atmospheric CO_2 trend over the shorter period from 1959 to 1969. Empirical β values ranging from 0.5 to 0.75 were obtained from experiments with a variety of single plants under greenhouse conditions and an unlimited supply of CO_2 at a concentration of 340 ppmv (Gates, 1985). At 680 ppmv, the β values decreased to 0.3 to 0.5. Reverse calculation of the logarithmic beta function of Bacastow and Keeling (1973) using TOTEM results shows that during the 300 yrs of TOTEM simulation, the β factor varies from close to zero to 0.7, well within the range of experimental and theoretical values.

It should be pointed out that currently there is no clear understanding of the *long-term* effect of increasing CO_2 on terrestrial photosynthetic uptake at the ecosystem and global levels. In contrast, the *short-term* response of terrestrial gross photosynthetic uptake to increasing atmospheric CO_2 is well documented (Eamus and Jarvis, 1989; Mousseau and Saugier, 1992; Allen Jr., and Amthor, 1995; Schimel, 1995; Wullschleger, Post, and King, 1995; Melillo and others, 1996a). Experimental studies of crop and non-cropland plants grown in doubled CO_2 atmospheres have shown growth rates ranging from −43 to +375 percent, with the median response falling within the range of +15 to 71 percent (Poorter, 1993; Ceulemans and Mousseau, 1994; Idso and Idso, 1994; McGuire, Melillo, and Joyce, 1995). However, in their interpretation of results from controlled-exposure experiments within the context of global C models, Wullschleger and others (1995) concluded that the link between gross photosynthetic uptake and rising atmospheric CO_2 concentrations has been limited at best. Simple information needed in the models, including TOTEM, to verify or refute even the most basic of assumptions, specifically on the role of changing atmospheric CO_2 on the gross photosynthetic uptake flux, may not all be addressed in the experimental studies. In extrapolating experimental results to the global carbon cycle, many more factors need to be considered, such as extrapolation of single-plant responses to heterogeneous biomes; interactions with light, soil moisture, and nutrient availability; ecological adaptations; and competitive interactions between various species and life forms. Thus, it is not surprising that the CO_2 fertilization effect on land plants has been interpreted in several different ways. Given the sensitivity of modeling calculations, including those of TOTEM, to the choice and functional relationships of the biotic growth factor, it is important to recognize that there are fundamental uncertainties involved in using results from controlled-exposure experiments, such as those cited above, to estimates of a global biotic growth factor.

Other climatological factors that have been observed to affect changes in Earth's processes were not considered in the present model analysis, such as changes in global mean precipitation and soil moisture. To date, however, there is no observational record showing that global precipitation has changed significantly in recent centuries, although its variability might have increased (Bradley and others, 1987; Diaz, Bradley, and Eischeid, 1989). In certain regions, such as North America, there are equivocal historical data indicating an increase in precipitation during the 20th century (Dai, Fung, and Del Genio, 1997).

IIA2. Land-use activities.–Prior to the start of the Industrial Revolution about the year 1850, land-use activities were primarily those of wood-fuel combustion for food preparation, heating, construction, biomass burning for metal and clay pottery production, and forest clearing for agricultural land-use. At the present time, these activities include the conversion of land for food production (grazing land, agricultural land), for urbanization (building human settlements, roads, and other structures), for energy development and supply (building dams, hydroelectric plants, and mining of fossil fuels), and for resource exploitation (mining of metals, harvest of forest hardwood) (Mackenzie, 1998). The consequences of these actions for Earth's natural resources and makeup of the land are manifested by increased deforestation, reforestation, logging, shifting cultivation, desertification and salinization, local flooding, loss of wetlands, and changes in the chemical and biological properties of aquatic systems (Meyer and Turner, 1994). The effect of changing land-use activities on Earth's processes is modeled in TOTEM via three mechanisms: First, as a direct perturbation when CO_2 derived from land-use changes is emitted to the atmosphere, and inorganic nutrients are released to the continental reservoirs; Second, as a negative feedback mechanism to rising atmospheric CO_2 concentrations; Third, as a major mechanism of material transfer from land to the coastal zone owing to soil erosion, mineral dissolution, and surface water runoff.

The first mechanism represents the enhanced conversion of organic phytomass and soil humus to its inorganic components when humans change the makeup of the land. For example, the conversion of forests to agricultural land releases CO_2 to the atmosphere through burning and decay and seasonal accumulation of C in crops. The release of CO_2 is accompanied by the release of N, P, and S in the same elemental ratios as those in phytomass or soils. This mechanism represents an enhanced source of CO_2 to the atmosphere and of nutrients N, P, and S to the continental reservoirs.

The rate of CO_2 emission to the atmosphere from land-use activities is an input function in TOTEM. The sources of the data used are discussed in section IIB on initial conditions and forcings. The fraction of the land-use emission flux originating from the phytomass is designated as f_{LU} and the fraction originating from the humus and dead organic matter reservoir is $(1 - f_{LU})$. Results of a model sensitivity analysis show a better fit of the historical atmospheric CO_2 data when 75 percent of the land-use CO_2 emissions is derived from the humus and 25 percent is derived from the phytomass (Ver, 1998).

The rates of release of nutrients N and S from the terrestrial phytomass to the continental soilwater reservoir owing to land-use activities are calculated by applying the appropriate C:N:S:P ratio for terrestrial biomass on the land-use flux of carbon, CF_{1LU} (parameters in the equations are defined in app. A; see also section IIB2):

$$\begin{aligned} CF_{1LU}(t) &= C_{LU}(t) \times f_{LU} \\ NF_{1LU}(t) &= C_{1LU}(t)/(C{:}N)_{1resp} \\ SF_{1LU}(t) &= C_{1LU}(t)/(C{:}S)_{1resp} \end{aligned} \tag{7}$$

Enhanced release rates from the humus reservoir to the continental soilwater are similarly calculated using the C:N:S:P ratio for humus and the land-use flux of carbon from humus, CF_{2LU}:

$$\begin{aligned} CF_{2LU}(t) &= C_{LU}(t) \times (1 - f_{LU}) \\ NF_{2LU}(t) &= C_{2LU}(t)/(C{:}N)_{2resp} \\ SF_{2LU}(t) &= C_{2LU}(t)/(C{:}S)_{2resp} \end{aligned} \tag{8}$$

The release of phosphorus from the terrestrial organic reservoirs takes into account the poorly soluble nature of most of the phosphorus compounds occurring in soil and the rapid immobilization of soluble inorganic phosphorus. Phosphorus quickly becomes unavailable for plant uptake after it precipitates out as poorly soluble iron, aluminum, and calcium phosphates or by occlusion with clay minerals (Brady and Weil, 1996). Studies have shown that repeated application of fertilizer P to croplands saturates the P-fixation capacity of the soil, thus contributing to an apparent long-term buildup of P in the continental soilwater reservoir. In TOTEM, the process of partitioning of soil phosphorus is represented by the parameter $fP_{LU\ react}$, that is the fraction of phosphorus remineralized in land-use that remains in the reactive inorganic form; the remaining fraction $(1 - fP_{LU\ react})$ is immobilized. Results of sensitivity analysis (Ver, 1998) indicate the best-fit values for $fP_{LU\ react}$ are:

$$\begin{aligned} fP_{LU\ react} &= 0.7; \quad 1700 < t < 1930 \\ &= 1.0; \quad t > 1930 \end{aligned} \tag{9}$$

The rates of release of P from the terrestrial phytomass and humus reservoirs to the continental soilwater are calculated as (parameters in the equations are defined in app. A);

$$\begin{aligned} PF_{1LU}(t) &= C_{1LU}(t) \times fP_{LU\ react}/(C{:}P)_{1resp} \\ PF_{2LU}(t) &= C_{21LU}(t) \times fP_{LU\ react}/(C{:}P)_{2resp} \end{aligned} \tag{10}$$

The negative feedback response to the land-use perturbation is a consequence of the release of CO_2, N, and S gases to the atmosphere and of the enhanced remobilization of N, P, and S to the continental soilwater reservoir. The increased availability of nutrients in continental soil-water, coupled with rising atmospheric CO_2 and warming temperatures, stimulates terrestrial productivity and storage of organic carbon in the terrestrial biota, thus increasing the drawdown of atmospheric CO_2. For example, when humus material with an average molar C:N:P ratio of 140:10:1 is mineralized, the remobilized N and P can ideally support growth of plant matter with an average C:N:P ratio of 510:4:1. Consequently, an additional 370 moles of the required C can be sequestered from the atmosphere through this recycling process. Of the 6 moles of excess N remaining in the continental soilwater reservoir, about 5.5 moles are eventually lost from the terrestrial realm to the atmosphere through denitrification and about 0.5 moles are transported to the coastal zone by rivers.

Land-use activities affect the rates of transfer of materials from land to the coastal zone when repeated tilling and loss of soil protective cover render the land more susceptible to soil degradation, particularly soil erosion (Houghton, 1983; Schlesinger, 1997; Brady and Weil, 1996). Soil erosion and water runoff contribute to the increased transport of particulate organic matter, and dissolved organic and inorganic C, N, P, and S to the coastal zone and to continental reservoirs, such as lakes and river flood plains (Mulholland and Elwood, 1982).

The effect of land-use activities on soil degradation and erosion is expressed in the fractional change in the process rate, f_{LUR}, and applied to the flux equation from soil to rivers (app. A). In the model, we assume that the temporal variation of this perturbation

follows that of the effect of land-use activities on the emissions of CO_2 to the atmosphere. Thus the temporal trend in soil degradation and erosion can be simulated by the trend in land-use CO_2 emissions to the atmosphere (see section IIB2 on land-use activities). To calculate the values for f_{LUR}, we applied a mathematical transformation on the land-use CO_2 emissions function such that the endpoints of the soil degradation and erosion perturbation function had a value of 0 at initial time 1700 and of 1 in the year 1995. The application of this function to the rate of soil degradation and erosion gives rise to a fractional increase in soil erosion with increasing human activities on land, followed by enhanced delivery to the coastal zone of terrestrially derived materials via the rivers. Using this relationship for soil degradation and erosion leads to about a doubling in the fluxes of particulate organic C, N, and P to the coastal margin via rivers between the years 1700 and 1995 in the standard TOTEM simulation. This result is in accord with literature data suggesting that the present fluxes of organic carbon, N, and P are approximately double pristine flux values (Meybeck, 1982; Milliman and Meade, 1983; Wollast and Mackenzie, 1989).

IIA3. Ocean-atmosphere exchange.–At the ocean-atmosphere interface, CO_2 gas exchange is assumed to occur instantaneously to achieve chemical equilibrium. The atmosphere above the ocean surface and the coastal and surface ocean reservoirs are considered in the model as well-mixed reservoirs, such that CO_2 is uniformly distributed within the entire reservoir. The seawater buffer mechanism allows a fractional change in total CO_2 in the surface-ocean mixed layer relative to that in the atmosphere. This partitioning was first introduced by Bacastow and Keeling (1973) and is known as the Revelle function, $R(C_{10})$;

$$R(C_{10}) = \frac{[C_{10}(t)/C_{10t=0}] - 1}{[C_7(t)/C_{7t=0}] - 1} \tag{11}$$

The Revelle function is also calculated as;

$$R(C_{10}) \approx R_0 + \{d \times ([C_{10}(t)/C_{10t=0}] - 1)\} \tag{12}$$

The value of the Revelle factor R_0 is 9, and d is a constant equal to 4; incremental changes in the Revelle function due to changes in the atmospheric CO_2 concentration are expressed by the last term on the right hand side of eq (12). Combining and rearranging eqs (11) and (12) yield an equation of the form expressing the time rate of change of the mass of carbon in the surface ocean reservoir as a function of the mass of carbon in the atmosphere;

$$\frac{dC_7}{dt} = \left\{ \begin{array}{c} \dfrac{C_{7t=0}}{R_0 C_{10t=0} + d \times [C_{10}(t) - C_{10t=10}]} \\ - \dfrac{C_{7t=0} \times [C_{10}(t) - C_{10t=0}] \times d}{\{R_0 C_{10t=0} + d \times [C_{10}(t) - C_{10t=0}]\}^2} \end{array} \right\} \times \frac{dC_{10}}{dt} \tag{13}$$

A similar derivation is obtained for the flux of CO_2 across the atmosphere-coastal ocean interface, with C_4 replacing C_7 in eq (13) (see app. A).

IIA4. Ocean mixing.–Carbon exchange between the surface mixed layer and the deeper ocean is a function of the carbon concentration difference between the surface and the deep ocean layers and the time needed to disperse an ocean surface perturbation into the bulk oceans, τ. The carbon concentration difference results from changes in C concentration owing to primary production, oxidation of sinking biogenic detrital matter below the photic zone, and changes in the dissolved inorganic carbon concentration in the surface layer induced by invasion of anthropogenic CO_2. The exchange of carbon

between the mixed surface layer and the deep ocean is modeled using an equation proposed by Revelle and Munk (1977);

$$\frac{d}{dt}\left(\frac{C_9}{h_9}\right) = \frac{(C_7/h_7) - (C_9/h_9)}{\tau_9} \tag{14}$$

where $h_7 = 100$ m and $h_9 = 3900$ m are the mean depths of water in the surface ocean and deep ocean reservoirs, respectively, and $\tau_9 = 500$ yrs. This equation enables the exchange flux between the mixed layer and deep ocean to be responsive to both the increase of CO_2 in the mixed layer as well as the changing concentration of dissolved inorganic carbon (DIC) in the deep layer. Results from models using more complex mathematical representations of ocean mixing (Hudson, Gherini, and Goldstein, 1994; Friedlingstein and others, 1995) do not differ substantially from TOTEM results.

IIB. Initial Conditions and Forcings

We begin analysis of the behavior of the carbon cycle under human perturbations prior to the year 1700 with the Earth system in an assumed steady state. This initial state is defined by the reservoir masses, transport fluxes for each element, and other reaction and transport parameters (table 1A-C; fig. 1; app. A). A major difference between TOTEM and other terrestrial ecological models and global circulation (climate) models (GCMs) is in the treatment of the observed atmospheric CO_2 concentrations. In most models of global environmental change (for example, Bruno and Joos, 1997; Cao and Woodward, 1998a; Sarmiento and others, 1998), the data on the atmospheric CO_2 concentrations are used as a prescribed input function. In TOTEM, however, the time course of change of atmospheric CO_2 concentration is not an input function, but–significantly to the results of our analysis–it is the output of model computations based on its mechanisms and external forcings of the past 300 yrs.

The assumption of the Earth system in a steady-state condition defined by the pre-industrial reservoir masses and fluxes establishes a base line in the model for the analysis of the effects of human perturbations and environmental stresses. This assumption is appropriate because the pre-industrial period, generally defined as the decadal to century time interval prior to the mid-1800s, was in a quasi-steady state under a small but sustained global human disturbance of the environment. For example, the estimated rates of release of CO_2 and CH_4 to the atmosphere associated with pre-industrial human activities of land use and wood-fuel combustion were almost constant over a period of 500 yrs prior to 1700. In the year 1200, the land-use CO_2 emissions were estimated as about 33×10^{12} moles C/yr, increasing only by 0.06 percent/yr to the year 1700 (Kammen and Marino, 1993). Fossil fuel emissions were negligible during this period (Keeling, 1973b), the Earth was about to enter a period of recovery from the lower global temperature of the Little Ice Age, and atmospheric CO_2 levels were relatively low (Barnola and others, 1995; Etheridge and others, 1996). Indeed, measurements from ice cores show that the concentration of atmospheric CO_2 over a period of about 1000 yrs prior to 1800 and including the pre-industrial era varied by no more than 10 ppmv, indicating that the global carbon cycle was approximately in a steady state (Raynaud and Barnola, 1985; Siegenthaler and others, 1988).

In our analysis, the steady state of the system is perturbed by five forcings owing to changes in human activities and in a climatic variable, affecting the major pathways of the C, N, P, and S cycles (fig. 2, Smil, 1985; Charlson, Anderson, and McDuff, 1992; Caraco, 1995; Galloway and others, 1995; Houghton and others, 1996; Marland and others, 1998). Four of these forcings are due to human activities: (1) gaseous emissions from fossil fuel burning (and other activities, such as the more recent activity of cement production), (2) land-use activities, (3) application of N and P inorganic fertilizers to

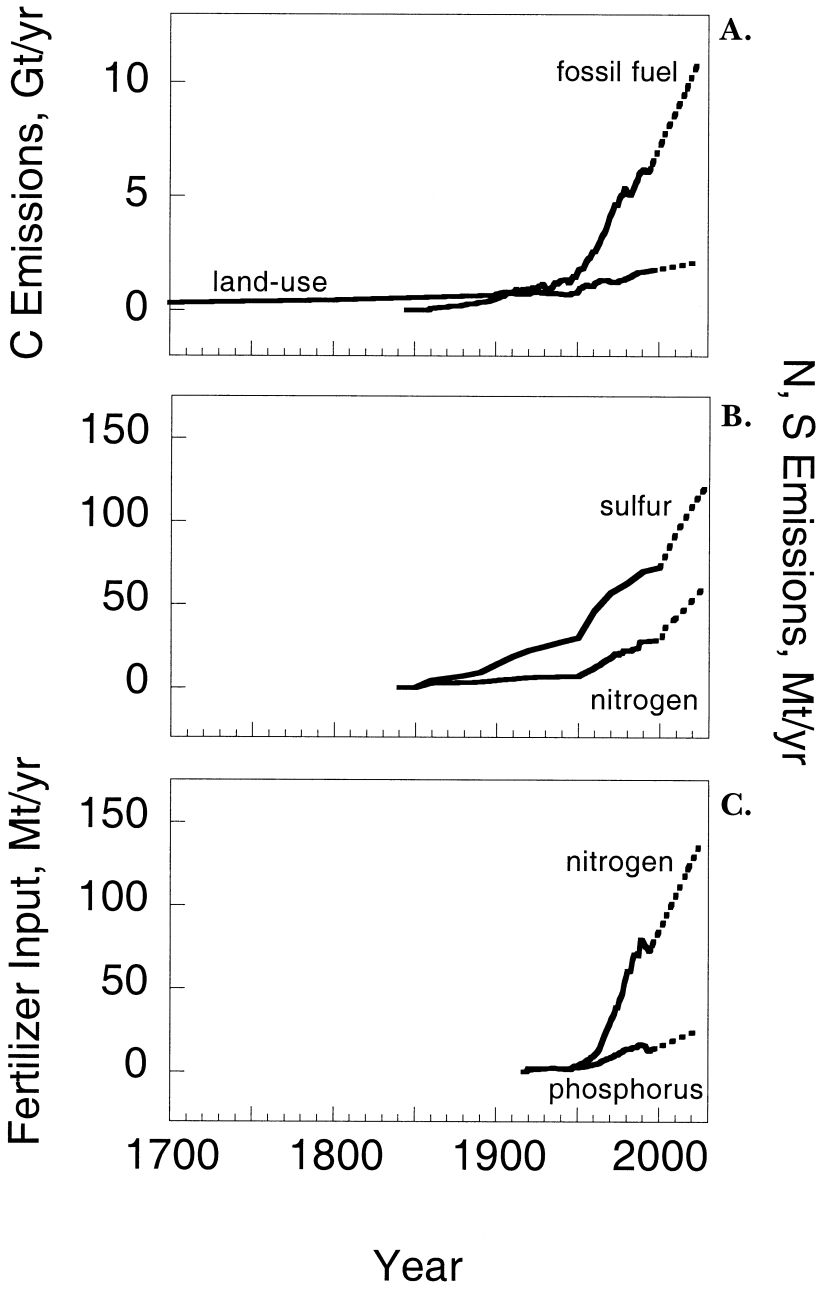

Fig. 2. Perturbations on Earth system simulated by TOTEM: (A) CO_2 and (B) N and S emissions from fossil fuel burning and land-use activities; (C) inorganic N and P fertilizer application;

croplands, and (4) disposal of municipal and industrial sewage. The fifth forcing is due to a change in a global climatic variable, the mean temperature of the Earth's surface. These forcings are input functions in TOTEM. Here, we describe the data sources and discuss briefly how these input functions are integrated into the TOTEM structure.

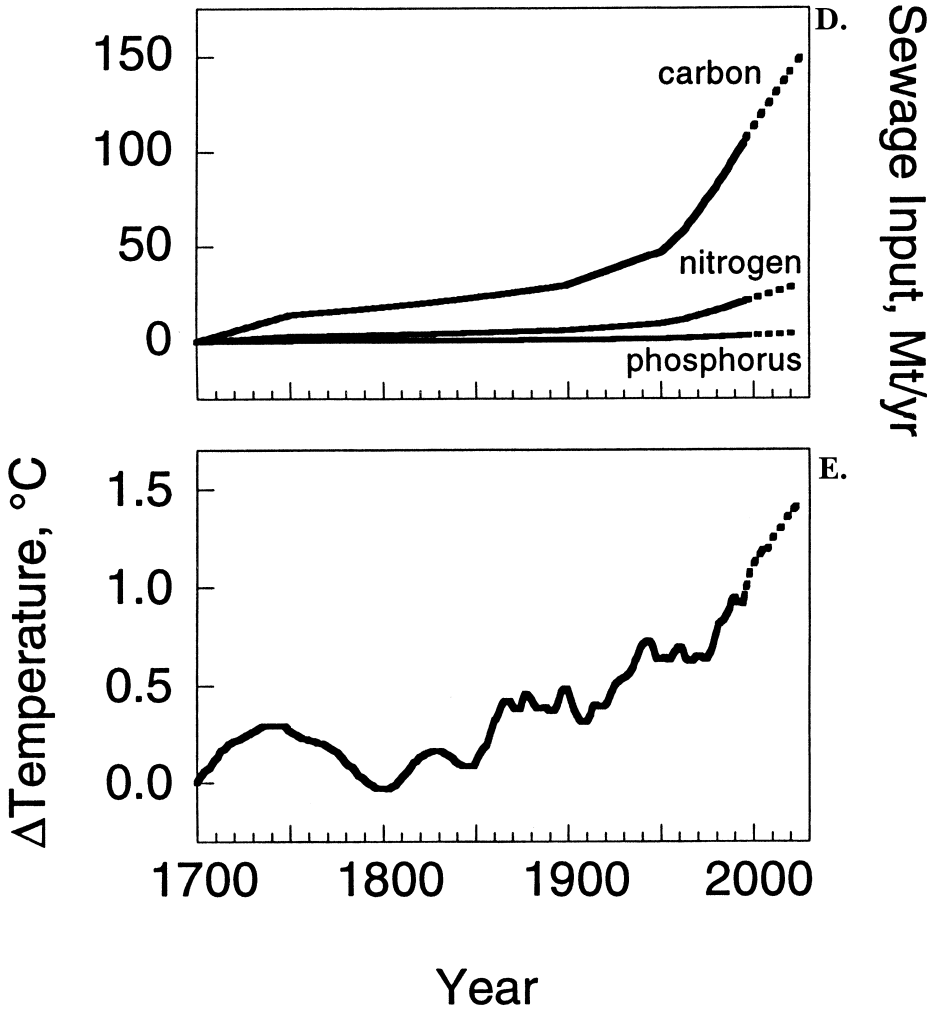

Fig. 2(D) municipal sewage and wastewater disposal; and (E) mean annual temperature variation. See text for description and sources of data.

IIB1. Emissions of gaseous C, N, and S from fossil fuel burning and other activities.–The annual global CO_2 emissions from fossil fuel burning and cement production for the period 1860 to 1995 are based on the estimates by Marland and others (1998). Global emissions of gaseous nitrogen-oxides (NO_x) and sulfur-oxides (SO_x) are based on estimates for the period 1860 to 1994 and extrapolated to 1995 (Dignon and Hameed, 1989; Dignon, 1992; Hameed and Dignon, 1992; Brown, Renner, and Flavin, 1997). On the decadal to century time scale, the anthropogenic emissions of C, N, and S gases are treated as external inputs to the atmosphere in our model. Fossil fuel CO_2 is injected into the atmosphere according to its emissions history and becomes part of the well-mixed atmospheric C reservoir. The prescribed boundary conditions for fossil fuel emissions are described by the function $C_{FF}(t)$ in units of 10^{12} moles C/yr (section IIA, fig. 2, app. A).

The fate of anthropogenic N and S in the atmosphere, however, is controlled by the very short lifetimes of these gases and their conversion products in the atmosphere. The

nitrogen component does not mix with the large N_2 reservoir but is deposited onto the terrestrial and coastal ocean reservoirs by wet and dry deposition and sedimentation of large particles. This flux is superimposed on the natural fluxes of N out of the atmosphere (fig. 1, app. A). Anthropogenic sulfur gases emitted to the atmosphere are also rapidly deposited onto terrestrial and oceanic surfaces. The partitioning of the deposition of the anthropogenic N and S products from the atmosphere on terrestrial and oceanic surfaces is based on the studies of long-range transport of these compounds (Logan, 1983; Bischoff, Paterson, and Mackenzie, 1984; Levy and others, 1990). In TOTEM, the fraction of anthropogenic N deposited onto the coastal ocean zone is $f_{NFF} = 0.4$, and that of anthropogenic S is $f_{SFF} = 0.5$. The remaining fractions of anthropogenic N $(1 - f_{NFF})$ and S $(1 - f_{SFF})$ are deposited directly on the land surface.

IIB2. Land-use activities.–The primary effect of land-use activities on the terrestrial organic reservoirs is prescribed by the time course of net C emissions to the atmosphere, $C_{LU}(t)$ (app. A). Kammen and Marino (1993) estimated the C emissions for the period 1700 to 1850 based on historical data for the pre-industrial, non-fossil fuel CO_2 emissions. Estimates by Houghton (1983; 1991a,b) for the more recent (1850-1990) land-use activities are reported as net CO_2 emissions, including the drawdown or release of CO_2 from such processes as conversion of forest to agricultural land, abandonment of agricultural land, harvest, and regrowth. Emission estimates for the period from 1990 to 1995 were extrapolated linearly from that of 1990 (Houghton, 1991b). The non-fossil fuel emission estimates used in TOTEM for the period 1800 to 1930 are consistent with those deduced from a deconvolution of high-precision ice core data from the Law Dome site in Antarctica (Bruno and Joos, 1997) and from atmospheric ^{13}C and ^{14}C data (Joos and Bruno, 1998). The parameters describing the effects of land-use activities in TOTEM were discussed in section IIA2.

IIB3. N and P inorganic fertilizer application.–The time course of this agricultural perturbation is based on data for the global consumption of inorganic fertilizer N and P from the United Nations Food and Agricultural Organization (United Nations FAO, various years) for the years 1950 to 1995. For data pre-dating the FAO collection (1917-1949), we used the estimates by Smil (1991). No provision for organic fertilizer application is included in the present version of the model. In TOTEM, fertilizer application is an external input to the N and P biogeochemical cycles because the residence times of N and P in their source reservoirs of atmosphere and crustal rocks, respectively, are much longer than the decadal to century time scales we consider. Only the fraction of applied fertilizer that is not assimilated by crops is considered as a forcing in the model. Although it is recognized that the partitioning of fertilizer N and P following its application to agricultural soils is very specific to the agricultural site, soil, and plant crop, we maintain the simplifying assumption of a global average condition that is consistent with the definition of the global reservoirs in the model. The partitioning used in TOTEM is based on estimates by Smil (1991): 45 percent of applied nitrogen fertilizer is converted to crop biomass, and the remaining 55 percent is the perturbation on the cycle. Of this fraction, at least 25 percent is transported to the coastal zone with surface runoff, 20 percent is volatilized to the atmosphere, and 10 percent is either stored in the soil or leached into the continental soilwater or groundwater reservoirs.

The partitioning of the fertilizer P in TOTEM differs somewhat from the partitioning of N: more of the applied phosphorus fertilizer (about 70 percent of the total) constitutes the perturbation after its partial assimilation by crops. Of this fertilizer P, most (about 50 percent of the total) is quickly rendered unavailable for plant uptake by precipitating out as insoluble iron, aluminum, and calcium phosphates or by occlusion with clay minerals. About equal amounts are transported with surface runoff (10 percent) and leached into the continental soilwater (10 percent) (Smil, 1991). Unlike N, there is no gaseous loss of fertilizer P. The unreactive P fraction is returned to the inorganic soil

reservoir where it may be either weathered back into the dissolved phase or transported in solid form to the coastal zone or continental environment. The potential for the unlimited increase in storage of P in the inorganic soil reservoir is counteracted by the first-order dependence of the weathering and runoff export fluxes to the size of the soil reservoir. The effect of temperature change on the weathering flux is small because the change in temperature over the past 300 yrs was only about 1°C.

IIB4. Sewage disposal.–In TOTEM, we assume that the global average sewage load is discharged into the coastal zone without undergoing any sewage treatment process. Following the analysis of Billen (1993) and Caraco (1995), we calculate the loading of municipal sewage into the coastal zone, in units of moles of organic C and total N and P/yr, using a globally averaged C, N, and P content of sewage and an average per capita rate of discharge applied to the global population (United Nations Population Division, 1995). Detergent phosphates are assumed to originate from urban industrialized regions (Caraco, 1995), where very little P is removed by wastewater treatment (Esser and Kohlmaier, 1991). Thus detergent-P is ultimately discharged into the coastal zone in the inorganic phosphate form. We calculate the global loading of detergent P into the coastal waters using an average per capita consumption rate applied to the urban industrialized population (United Nations Population Division, 1995).

The cumulative amounts of organic C and total N and P added by sewage discharges to the coastal zone, as defined in the model pathways (fig. 1), have been small relative to the other perturbations so far. However, continuing growth of the human population that produces sewage and detergents at the same rates as at present may result in a stronger fertilization of the coastal zone in the future. Conversely, different pathways of discharge of untreated sewage and other products of human perturbations on land may lead to consequences that are outside the present analysis of TOTEM. For example, discharges of municipal sewage and detergent may go into riverine systems where increased organic matter production and adsorption onto suspended and bedload sediments may occur, and where both detrital and newly formed organic matter may be stored for at least decades to centuries, in part delaying their transport to the coastal zone and in part contributing to the conversion of organic C and N into inorganic forms in the storage areas.

IIB5. Temperature.–The mean global temperature history of the Earth for the period 1700 to 1995 was derived from data given in UCAR/OIES (1991), by Nicholls and others (1996), and by Houghton and others (1996). For the terrestrial realm, temperature and availability of water are two of the most important climatic variables. At present, large variations in mean annual temperature (or mean temperature of the growing season) and water balance, as reflected in net precipitation, characterize the continental environment. In this model, the response of the global ecosystem to changes in temperature is through the biologically mediated processes of photosynthesis, plant and soil respiration, and denitrification on land, and the inorganic process of rock weathering. Because the temperature change between 1700 to the late 1990s was only about 1°C, the response of Earth system processes to this perturbation was small (see discussion of eq (6) in section IIA1).

III. CARBON RESPONSE TO PERTURBATIONS

In the global model of the carbon cycle that is perturbed by four human forcings and global temperature rise (figs. 1, 2), carbon is redistributed among the reservoirs in the domains of land, atmosphere, coastal ocean, and open ocean. The first verification of the model TOTEM is a comparison of its results for the carbon cycle with the well-established record of the rise in atmospheric CO_2 concentrations. The model results for the past 300 yrs compare very well with observational data (fig. 3) and with results from other models addressing the partitioning of anthropogenic CO_2. The major constraints

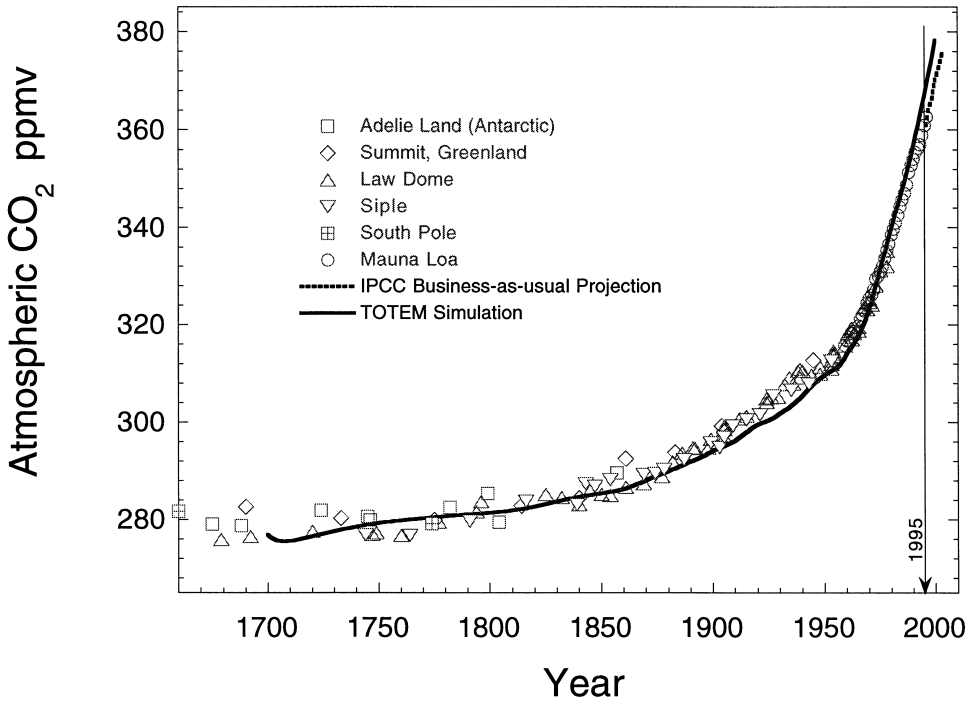

Fig. 3. TOTEM simulation of the rise in atmospheric CO_2 during the past 300 yrs compared with the observational data from ice cores taken at East Antarctica, Siple, and South Pole stations, and measurements made at the Mauna Loa Observatory, in units of ppmv CO_2. Note the very good correspondence between TOTEM results and the proxy and direct atmospheric measurements for the past 300 yrs.

on the presently accepted CO_2 budget for the past 300 yrs are the combined observed atmospheric CO_2 data obtained from ice cores (Neftel and others, 1985; Friedli and others, 1986; Barnola and others, 1995; Etheridge and others, 1996) and from Mauna Loa (Keeling and Whorf, 1998). Model results for the decade of the 1980s are also in agreement with observational data. There is very close agreement between the TOTEM-calculated rates for 1985 with the values reported in the literature as average rates for the period 1980 to 1989. For example, the TOTEM-calculated anthropogenic CO_2 accumulation in the atmosphere (3.4 Gt C/yr, table 2, column for 1985) is consistent with direct measurements or estimates of atmospheric CO_2 accumulation (avg of 3.3 ± 0.2 Gt C/yr) (Sarmiento, Orr, and Siegenthaler, 1992; Houghton and others, 1996). The calculated TOTEM rate of oceanic accumulation for the same year (1.9 Gt C/yr) is the same as that predicted from ocean-atmosphere models (1.9 Gt C/yr for 1980-1989) (Siegenthaler and Sarmiento, 1993) and within the range of estimates of the oceanic sink as inferred from analysis of changes in oceanic and atmospheric $^{13}C/^{12}C$ ratios, giving an average of 2.1 ± 0.9 Gt C/yr over the period 1970 to 1990 (Quay, Tilbrook, and Wong, 1992).

R. F. Keeling and others (1996) recently estimated the enhanced uptake of CO_2 for the period 1991 to 1994 by the Northern Hemisphere forests (2.0 ± 0.9 Gt C/yr) and by the global oceans (1.7 ± 0.9 Gt C/yr) from changes in atmospheric CO_2 concentration and atmospheric O_2/N_2 ratio. The rates calculated by TOTEM for 1992 fall within the range of these observed values: global terrestrial biotic uptake of 1.5 Gt C/yr and global oceanic uptake of 2.0 Gt C/yr. Finally, TOTEM results for the partitioning of anthropogenic CO_2 over the time course from 1850 to present (fig. 4) compare very well with

TABLE 2

Historical summary of carbon sources, sinks, and enhanced fluxes owing to human-derived perturbations and temperature change calculated from TOTEM. In column 2 are the initial values, in Gt C/yr, prior to the start of the perturbations. In columns 3–6 are the computed magnitudes of change from initial conditions, in Gt C/yr.

Carbon fluxes in background (pre-1700) and perturbed (1700–1995) states	Steady State Pre-1700	Magnitude of change since 1700			
		Pre-Industrial † 1860	Industrial § 1950	Post WW II * 1985	Recent 1995
Major Sources of Anthropogenic C:					
(1) Fossil fuel burning	0	0.09	1.64	5.42	6.24
(2) Land-use CO_2 emissions	0	0.58	0.79	1.57	1.76
(3) Sewage discharges	0	0.02	0.05	0.09	0.1
Major Sinks of Anthropogenic C:					
(4) Atmospheric accumulation ‡	0	0.32	0.88	3.44	4.52
(5) Oceanic accumulation ††	0	0.26	0.83	1.9	2.36
(6) Organic C in coastal sediments	0	0.02	0.05	0.11	0.13
(7) Net terrestrial gain (+) or loss (–) §§	0	-0.46	-0.05	0.15	-0.56
Fluxes Perturbed by Human Activities:					
(8) Terrestrial CO_2 uptake	0.60	0.13 (22%)	0.76 (127%)	1.82 (303%)	1.31 (218%)
(9) Oceanic CO_2 uptake (+) or loss (–)	-0.5	0.24 (48%)	0.79 (158%)	1.73 (346%)	2.16 (432%)
(10) Riverine DOC and POC	0.41	0.01 (2%)	0.02 (5%)	0.1 (24%)	0.12 (29%)
(11) Riverine DIC and PIC	0.56	0.02 (4%)	0.03 (5%)	0.14 (25%)	0.16 (29%)
(12) Carbonate accumulation	0.25	0.01 (4%)	0.01 (4%)	0.05 (20%)	0.06 (24%)
Long-term geologic fluxes:					
(13) Organic C burial in sediments	0.13				
(14) Carbonate C burial in sediments	0.4				
(15) Weathering	0.13				
(16) Volcanism and dust	0.10				
(17) Hydrothermal venting	0.06				
(18) Uplift of old C	0.37				

† Prior to the industrial revolution in 1860, the terrestrial reservoirs were a net source of anthropogenic CO_2 to the atmosphere from the extensive deforestation of Northern Hemisphere forests, and conversion of grassland to cropland and pasture land (Houghton, 1983). Most of this C accumulated in the atmosphere and oceans. The transfer of perturbation effects to the coastal zone via the rivers was minimal.
§The Industrial Revolution through early post-World War II (1860–1950) is highlighted by the development of a global fossil fuel-based economy (Marland and others, 1998).
* The post WW II era (1950–1995) is characterized by the extensive use of synthetic agricultural fertilizers and phosphate-based detergents. Increased transport of particulate and dissolved organic carbon to the global coastal zone has resulted in the increased accumulation of organic C in coastal sediments (6) by 100% of the long-term flux (13) of organic material by the year 1995 (column 6).
‡ For values in columns 3–6, Atmospheric accumulation = (1) + (2) − (8) − (9).
†† For values in columns 3–6, Oceanic accumulation = (3) + (9) + (10) + (11) − (6) − (12).
§§ For values in columns 3–6, Net terrestrial = (8) − (2) − (10). Negative values denote emission of CO_2 to the atmosphere.

results from GCM models (Sarmiento, Orr, and Siegenthaler, 1992; Bruno and Joos, 1997) and from models of the global carbon cycle (for example, Hudson, Gherini, and Goldstein, 1994). The agreement with other workers' observational and modeling results lends further credence both to their conclusions and to our Earth-system model for the land-ocean-atmosphere system.

Over the past 300 yrs, the largest perturbation on the Earth's surface system was the cumulative emission of about 440 Gt C to the atmosphere: 249 Gt C or 56 percent owing to fossil fuel burning and cement production and 193 Gt C or 44 percent from land-use

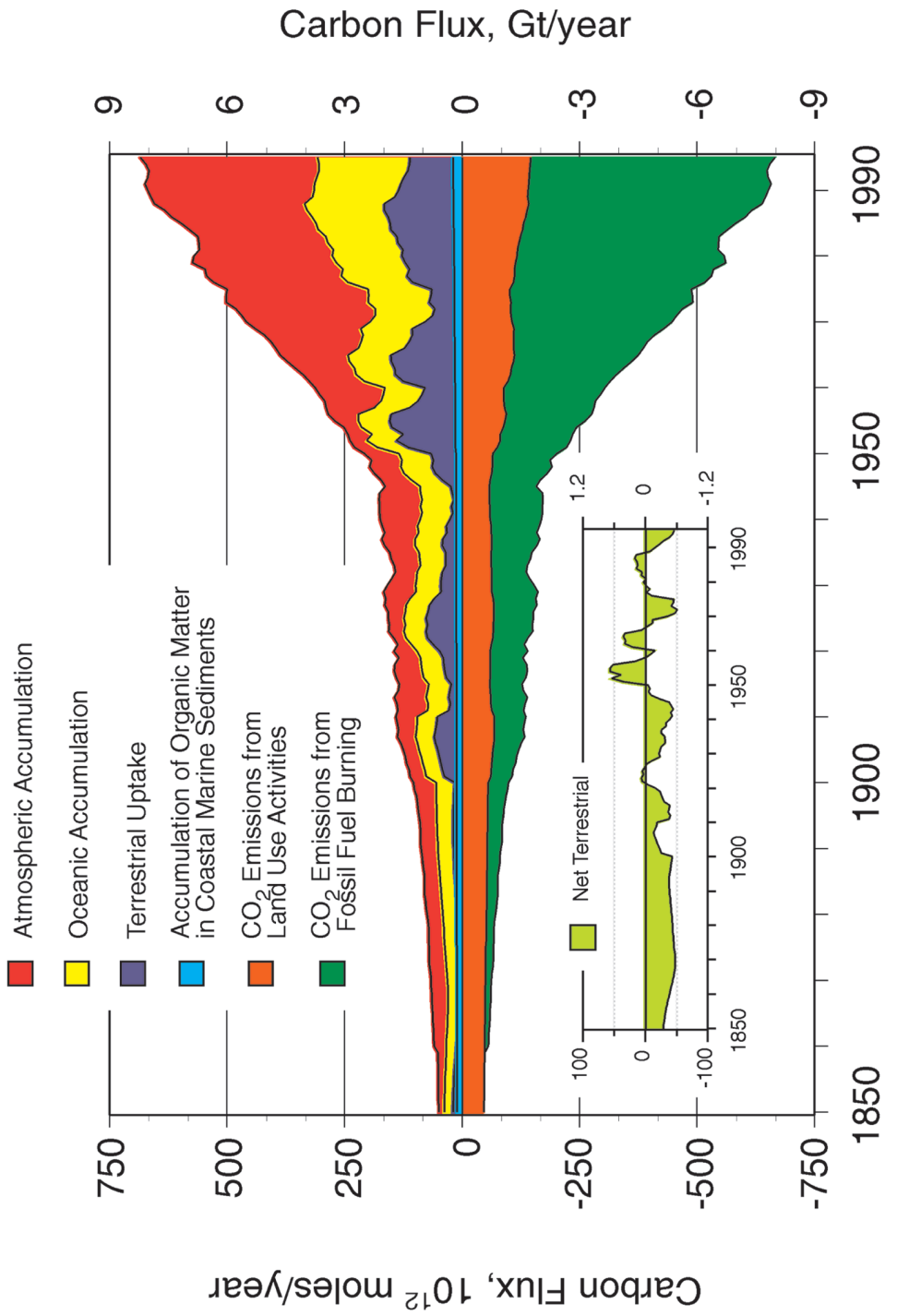
Carbon Flux, Gt/year
9
6
3
0
-3
-6
-9
Atmospheric Accumulation
Oceanic Accumulation
Terrestrial Uptake
Accumulation of Organic Matter in Coastal Marine Sediments
CO2 Emissions from Land Use Activities
CO2 Emissions from Fossil Fuel Burning
Net Terrestrial
100
0
-100
1.2
0
-1.2
1850
1900
1950
1990
Year
Carbon Flux, 10^12 moles/year
750
500
250
0
-250
-500
-750
1850
1900
1950
1990

Figure 4

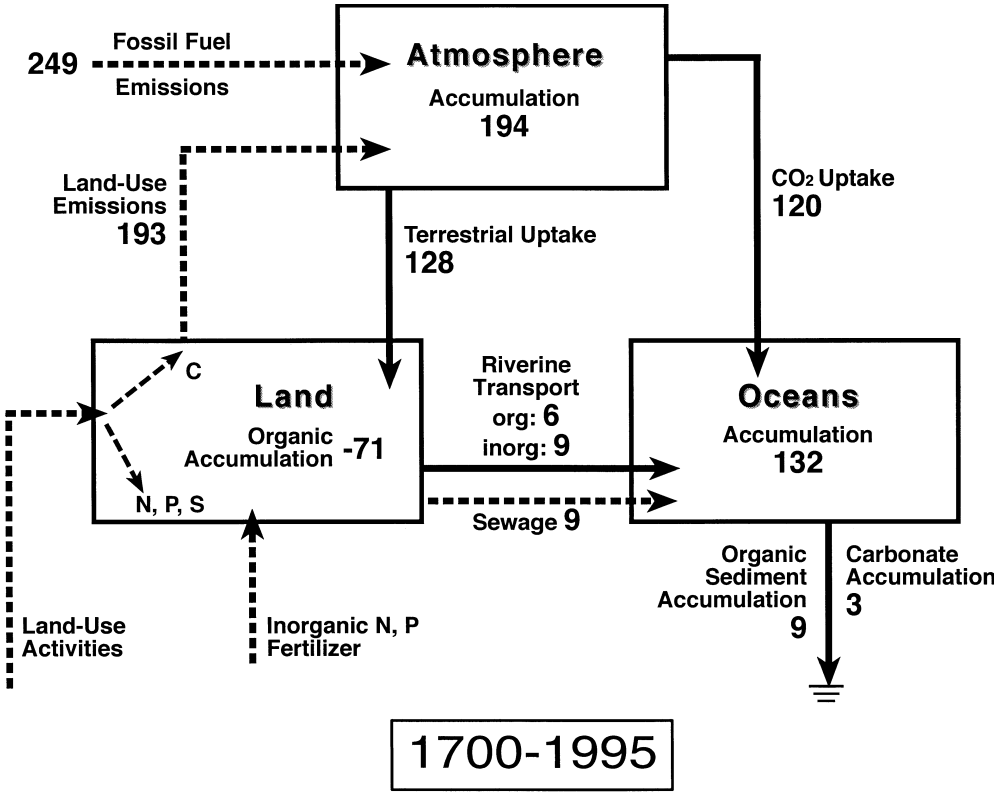

Fig. 5. Schematic diagram of the cumulative carbon sources and sinks over the past 300 yrs of perturbation from human activities and temperature variation. Masses and cumulative fluxes in Gt C.

activities (fig. 5). Smaller perturbations included the enhanced cumulative transport to the coastal zone of about 6 Gt organic C and 9 Gt inorganic C owing to land-use activities and the cumulative loading of about 9 Gt C from municipal sewage and wastewater. The cumulative response fluxes of C resulting from these perturbations included the uptake of about 120 Gt C by the global oceans and the fertilization of the terrestrial biotic reservoir of about 128 Gt C. The latter was due to rising atmospheric CO_2, inputs of N and P nutrients remobilized from land-use and from application of agricultural fertilizers, and warming temperatures. However the enhanced biotic uptake was greatly exceeded by the loss of mass from land-use activities (193 Gt C emitted to the atmosphere and 6 Gt C transported to the coastal margin), resulting in a net loss of about 70 Gt C from the terrestrial organic C reservoirs (phytomass and humus). The atmosphere accumulated about 195 Gt C, the oceans about 130 Gt anthropogenic C, and the coastal organic and inorganic sediments accumulated 12 Gt C.

One of the essential features of our analysis, using TOTEM, is a biochemical mechanism for the increased photosynthetic uptake by the terrestrial phytomass sus-

Fig. 4. The model-calculated partitioning of the annual carbon perturbation fluxes to the atmosphere for the period 1850 to 1995 in units of 10^{12} moles C/yr and Gt C/yr. The anthropogenic carbon sources are plotted on the (−) side and the resulting accumulations are plotted on the (+) side. Note that the values for CO_2 emissions from land-use activities are plotted separately from those for the enhanced terrestrial CO_2 uptake flux to highlight their opposing effects on the terrestrial organic reservoirs. The net accumulation (or loss) by the terrestrial organic reservoirs is plotted in the inset (see also table 2, footnote §§)

tained by an enhanced supply of N and P to soils. A major source of this input is the remobilization of N and P accompanying the emission of CO_2 to the atmosphere due to increasing human activities on land. Our results are consistent with the measured atmospheric CO_2 and O_2/N_2 data, forest inventories, and global carbon budgets (Keeling, Chin, and Whorf, 1996; Keeling, Piper, and Heimann, 1996; Houghton, Davidson, and Woodwell, 1998; Joos and Bruno, 1998) and provide an explanation for the concurrent release of CO_2 to the atmosphere and an accumulation of C in terrestrial ecosystems (Houghton, Davidson, and Woodwell, 1998). Interestingly, although the effect of land-use activities on nutrient remineralization has been mentioned in the literature (Melillo and others, 1993, 1996b), it has yet to be incorporated in many terrestrial-ecological models.

Our results support the suggestion made by several authors (Wofsy and others, 1993; Houghton, 1995) that the terrestrial phytomass was being fertilized during the decade of the 1980s (table 2, row 8, fifth column). TOTEM results also show that the terrestrial organic reservoirs, including the phytomass and soil humus, were a source of C via the emission of CO_2 from land-use activities (row 2, fifth column), sustaining a rough organic C balance within the terrestrial organic reservoirs (row 7, fifth column). During this period, it is clear that the terrestrial realm was not a net sink for anthropogenic CO_2 but rather a conduit for the transfer of the effects of the perturbation back to the atmosphere and to the adjacent coastal zone (fig. 4), and perhaps to the sediments of wetlands, lakes, ponds, and river floodplains (Mulholland and Elwood, 1982). The ultimate sinks for anthropogenic CO_2 during this recent decade were the atmosphere, the surface, and deep oceans, and, less importantly, the coastal sediments and aquatic systems on land.

Although TOTEM does not allow for discrimination of hemispheric variations in carbon sources and sinks, the results are consistent with a scenario where, in recent decades, enhanced terrestrial biotic uptake might be primarily occurring in Northern Hemisphere forests while carbon emissions from land-use activities could primarily come from deforestation taking place in the tropics. The temperate forests of Europe, North America, and Russia underwent extensive deforestation, changes in land-use patterns, and urbanization for most of the 18th through 20th centuries (Houghton, 1983). At least part of the nutrients remobilized owing to these deforestation activities may now be sustaining the CO_2-fertilization effect in these regions. Data collected by the UN FAO (1995) indicate that between 1981 and 1990, the global temperate forests and other wooded land increased in area by 0.1 percent (about 2 million hectares) while the forested area of the tropical region declined by 3.6 percent (about 98 million hectares). Most of the increase in temperate forest area occurred in the extensive forests of Russia and Canada in the Northern Hemisphere, while loss of tropical forest area was highest in Asia, Latin America, Africa, and the Caribbean. Observations during the late 1980s and early 1990s suggest that the Russian forests were accumulating 0.66 Gt C/yr (Kolchugina and Vinson, 1995).

According to an analysis of recent trends in the atmospheric concentrations of O_2 and N_2 (Keeling, Piper, and Heimann, 1996), the global terrestrial biota was a sink for anthropogenic CO_2 between 1991 and 1994. One implication is that tropical ecosystems were not a strong net source or sink for CO_2 during this period. Recent estimates by several studies show that during this same period, the global tropical regions were being deforested at an average rate equivalent to 1.2 to 2.3 Gt C/yr and undergoing enhanced biotic uptake at an average rate of 0.5 to 1.0 Gt C/yr (Polglase and Wang, 1992; Taylor and Lloyd, 1992; Houghton, 1995; Melillo and others, 1996b). TOTEM global calculated rates for the period 1990 to 1994 differ from those derived from the study by R. F. Keeling and others (1996) but are compatible with the estimates for the global tropical regions mentioned above. Our model shows for 1995 (table 2, column 6) that the global

terrestrial phytomass was being fertilized at an average rate of 1.31 Gt C/yr while losses due to deforestation and other land-use activities averaged 1.76 Gt C/yr. Thus the terrestrial organic reservoirs were a net source of CO_2 to the atmosphere at an average rate of 0.45 Gt C/yr (fig. 4, inset). The source of the discrepancy between the conclusions of TOTEM and those of others is not clear. Several aspects of our model may explain this discrepancy: TOTEM calculations include the release of CO_2 to the atmosphere from soil respiration, which effectively reduces the calculated global biotic uptake. Our results are also sensitive to the coupling between land-use emissions of CO_2 (Houghton, 1991b) and N and P remobilization, as discussed in the preceding sections. Model calculations show that a lower estimate of the land-use emission flux (1.1 ± 0.5 Gt C/yr in 1995, T. M. L. Wigley, personal communication) would result in a smaller net release of CO_2 by the terrestrial organic reservoir; however, when the lower land-use emissions flux is prescribed, the resulting TOTEM-calculated atmospheric CO_2 concentrations would be lower than those measured at Mauna Loa. It is also possible that some of this discrepancy may be accounted for by transient storage of organic carbon, derived from enhanced erosion of humus and soils, in such continental areas as lakes, ponds, dammed reservoirs, and river flood plains (Likens and others, 1981; Mulholland and Elwood, 1982; S. V. Smith, personal communication).

Melillo and others (1996a) attribute the difference between their estimates of carbon uptake by the terrestrial phytomass and those of R. F. Keeling and others (1996) to interannual variations in climate, which, except for changes in global temperature, are not addressed by our model. Indeed, carbon fluxes calculated by the Terrestrial Ecosystem Model (TEM; Tian and others, 1998) and the Frankfurt Biosphere Model (FBM; Kindermann, Wurth, and Badeck, 1996) show that the complex terrestrial biotic response to variations in temperature and precipitation in different latitudes and ecosystems contributes substantially to the atmospheric CO_2 anomaly on the interannual timescale. Results from a TEM simulation of the Amazonian ecosystems show that during El Niño years, these ecosystems were a net source of carbon to the atmosphere (up to 0.2 Gt C/yr in 1987 and 1992) while in other years, these ecosystems acted as a carbon sink (up to 0.7 Gt C/yr in 1981 and 1993). Additionally, recent analysis of decades of U.S. Forest Service data indicate that increased efficiency and improvements in forest technologies, various conservation strategies, and recycling, have contributed to revitalized forest growth in North America and Europe (Wernick, Waggoner, and Ausubel, 1997). Changes in these and other socio-economic factors are also not dealt with in TOTEM.

The use of data for the Amazonian tropical forests (Grace and others, 1995) to represent net CO_2 uptake by all the tropical forests of the world (Keeling, Piper, and Heimann, 1996) may also be a source of the discrepancy between the studies discussed above. Forest survey data collected by the UN FAO (1995) show that between 1990 and 1995 only about 45 percent of the global reduction in forest area occurred in South America while 55 percent of the reduction took place in Asia, Oceania, and Africa. Thus, while it is conceivable that the tropical forests in the Amazon basin might have been in carbon balance, the major tropical forests of the rest of the world were net sources of CO_2 to the atmosphere. Recent analyses by Melillo and others (1996a) show that in 1990, the tropical regions of the world were net sources of CO_2 to the atmosphere, within a relatively wide range of uncertainty of between 0.2 to 1.8 Gt C/yr.

IV. RESPONSE OF NITROGEN AND PHOSPHORUS TO HUMAN PERTURBATIONS

As discussed in the preceding sections, fertilization of the terrestrial biota was maintained by the combined effects of rising atmospheric CO_2, warming temperatures, and the enhanced supply of nutrient N and P remobilized during land-use activities. Most of the remineralized N enters the continental soilwater reservoir where it domi-

nates nitrogen inputs from other perturbations, such as agricultural fertilizers and atmospheric deposition. The finding that the effect of atmospheric N deposition was not a major factor in fertilization of the terrestrial biota is consistent with results from a recent ^{15}N-tracer study conducted in Northern Hemisphere temperate forests, which indicates that elevated nitrogen deposition rates are unlikely to be a major stimulant to C uptake by forests (Nadelhoffer and others, 1999). Our results for the recent decade of the 1980s indicate that of the total anthropogenic N and P inputs to continental soilwater, land-use activities accounted for 75 percent of N and 95 percent of P, while agricultural fertilizer application supplied 15 percent of N and 5 percent of P. Atmospheric deposition accounted for the remaining 10 percent of anthropogenic input of N into the continental soilwater reservoir.

Carbon storage in plants and humus on land may be limited by nutrients other than nitrogen. In particular, the availability of phosphorus may become critical, because the ultimate source of phosphorus for uptake by terrestrial plants is through the dissolution of phosphate minerals in soils and crustal rocks, a relatively slow process. In our model, by the decade of the 1980s, global continental soilwater P had declined to 29 µg/l from an initial concentration of 41 µg/l prior to 1700. This decline is a net result of increased biotic uptake, erosional loss, and surface runoff, relative to the inputs from mineral weathering, leaching of agricultural fertilizers, and remobilization from land-use. Survey findings by Brady and Weil (1996) show that 20 to 40 percent of global cropland and permanent pasture (1 to 2 billion hectares) contain P-deficient soils, limiting the growth of crops and native vegetation. Constrained by the residence time of phosphate minerals in soil and assuming no drastic changes in input and output fluxes, the continental soilwater P reservoir is projected to decline further and reach a new, lower steady-state level in about 4000 yrs. However, ecological adaptations to the impoverished nutrient content at this future time period could modify the response to such a change in certain key biochemical processes, such as photosynthesis and humus respiration.

The course of change of N in the continental soilwater reservoir differs from that of P because of the additional sources of N from atmospheric deposition, from humus recycling (that produces more N relative to that required for plant uptake), and from leaching of fertilizers. The remobilization of N from land-use activities is the largest anthropogenic perturbation on the continental soilwater N reservoir. Concentrations of N in soils, continental soilwater, and shallow groundwater reservoirs show increasing trends through 300 yrs of perturbation, consistent with observed data and global estimates (Smith, Alexander, and Wolman, 1987; Galloway and others, 1995; Brady and Weil, 1996).

The role of the C-N-P-S coupling in the control of the carbon cycle is demonstrated by the results of a numerical experiment, as shown in fig. 6A. In this experiment, the nutrients N, P, and S were decoupled from the effects of changing land-use practices that cause their increased transport from land to the soilwater reservoir and to the coastal zone by water runoff and soil erosion. Instead, the nutrients N, P, and S were allowed to remain in the land-domain reservoirs of humus, soil, and soilwater. This experimental condition transforms TOTEM into a model that is structurally very similar to several terrestrial-ecological models with respect to their treatment of land-use change (for example, Hudson, Gherini, and Goldstein, 1994; Friedlingstein and others, 1995; Cao and Woodward, 1998b).

The results of this decoupled-cycle scenario show a smaller rise in atmospheric CO_2 relative to that produced by TOTEM in the standard run with coupling and to the observed data from the polar ice cores and from Mauna Loa (fig. 6A). The divergence in results is greatest during the period when the temperate forests of Europe, North America, and parts of Asia were undergoing extensive deforestation, and grasslands were being converted to pasture and cropland (18th through early 20th centuries). It

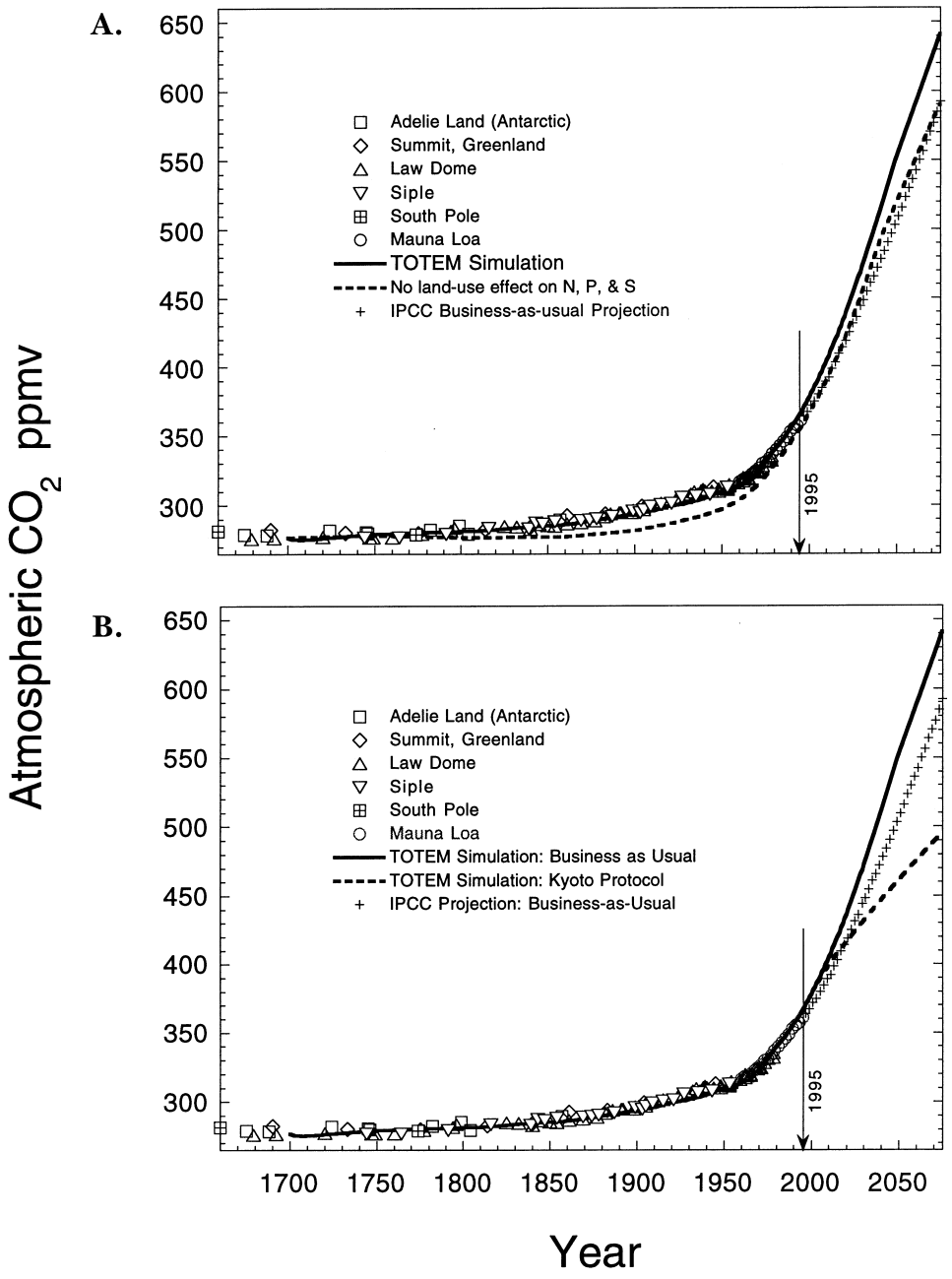

Fig. 6(A) The effect of decoupling the nutrients N, P, and S from C with respect to changing land-use practices on the mean concentration of global atmospheric CO_2 during the past 300 yrs and 80 yrs into the future. The results are compared with the observational data as described in figure 3. (B). Future projections of atmospheric CO_2 increase for three scenarios: Intergovernmental Panel on Climate Change "business as usual" (BAU, IS92a), TOTEM "business as usual," and TOTEM simulation for 1997 Kyoto Protocol reduced emissions. See text for further discussion.

appears from the results that the release of N and P from land-use practices, as treated in TOTEM, was a process in the overall control of atmospheric CO_2 concentrations. In the decoupled land-use scenario, more nutrients from the biological recycling and remineralization of humus were available for photosynthetic uptake, because the released organic N, P, and S on land were not lost to the coastal zone by water runoff and enhanced soil erosion owing to land-use change. Interestingly, results from this calculation for 1995 and beyond (fig. 6A) correspond very closely to those of the Intergovernmental Panel on Climate Change (IPCC) projections based on a scenario of "business as usual" (discussed in greater detail in a later section). This finding is important because it brings to question the validity of projections of atmospheric CO_2 using models that do not fully account for the complexity of biotic feedbacks. The future time course of atmospheric CO_2 is one of the most important variables in projections of the rate and magnitude of warming of the Earth's surface because of human activities.

V. RESPONSE OF THE GLOBAL COASTAL MARGIN

The global coastal margin occupies a small fraction of open ocean area (7-10 percent of total oceanic surface area) that has been heavily affected by human activities, disproportionately more than the rest of the oceanic realm. Here, we demonstrate how the coupled biogeochemical cycles interact to determine the changes over the past 300 yrs in the organic carbon balance in the coastal ocean and the net exchange of CO_2 between the coastal ocean surface layer and the atmosphere.

Prior to extensive human activities on land, the global coastal margin was likely in a near-steady state of net heterotrophy at a rate equivalent to about 0.08 Gt C/yr (Wollast and Mackenzie, 1989; Smith and Hollibaugh, 1993; see Ver, Mackenzie, and Lerman, 1999 for recent discussion on this conclusion). A system is heterotrophic when the gross consumption or oxidation of organic matter exceeds its in situ gross production. The accumulation of calcium carbonate in shallow-water, coastal margin environments was also a source of CO_2 to the atmosphere at that time (Wollast and Mackenzie, 1989). Thus the pre-industrial net flux of CO_2 between the coastal oceans and the atmosphere owing to organic and inorganic processes was a net evasion to the atmosphere of about 0.2 Gt C/yr (fig. 7). From the year 1800 to about 1900, human perturbations on land and annual temperature variations had only a slight net effect on the trophic status of the coastal zone. Between 1900 and 1940, there was a slight net tendency toward autotrophy (when gross production of organic matter exceeds gross respiration), which followed the pattern of change in land-use activities and greater input of nutrients N and P from land, indicating the importance of land-derived fluxes to the trophic status of the coastal zone. After 1940, the coastal zone became more heterotrophic, resulting from the increased delivery of dissolved and particulate organic carbon (DOC and POC) via the rivers to the oceans because of land-use activities. The computed trend toward increased heterotrophy during the past 300 yrs applies to the modeled global coastal ocean, regardless of the initial trophic state of the coastal zone (that is, either heterotrophic or autotrophic). The net exchange of gaseous CO_2 also followed the time course pattern of change of land-use activities, indicating the transfer of the effects of the perturbation from land to the neighboring domains. The effect of rising atmospheric CO_2 pressure opposing the flux of CO_2 from coastal waters to the atmosphere becomes increasingly evident after 1900, when fossil fuel consumption increased exponentially. The 1970 to 1980 decline in fossil fuel consumption, owing to the petroleum energy crisis, is reflected in a slight decline in the penetration rate of anthropogenic CO_2 into the coastal surface ocean.

Over the period of 300 yrs of human perturbation on land, the coastal margin maintained its state of heterotrophy and its pre-industrial role as a net source of CO_2 to the atmosphere owing to organic metabolism. The export of terrestrial organic matter and its consumption in the coastal zone increasingly exceeded in situ production. The

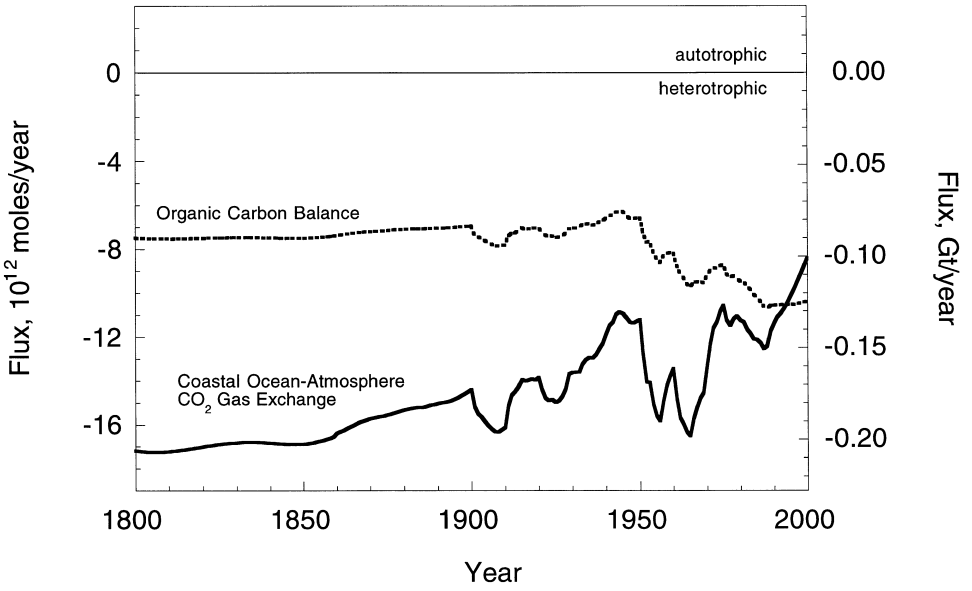

Fig. 7. Organic carbon balance (dashed line) and net exchange flux of CO_2 across the air-seawater interface (solid line) for the coastal margin system, in units of 10^{12} moles C/yr and Gt C/yr. Negative values indicate CO_2 flux out of the surface waters.

fate of this organic matter was remineralization to the DIC pool, burial in the coastal sediments, and, to a lesser extent, export to the continental slope. Although the riverine input of inorganic nutrients also increased significantly, the incremental new production enabled by them was apparently not sufficient to reverse coastal zone metabolism toward net autotrophy. Increased heterotrophy and carbonate precipitation in the coastal margin (fig. 7) are sources of dissolved inorganic C. The back-pressure created by the additional DIC appears to modulate the response of the coastal ocean to the stronger opposing pressure across the air-sea interface from rising atmospheric CO_2 concentrations. Thus the net effect of sustained heterotrophy and increased carbonate precipitation is a reduction in the potential sink-strength of the coastal ocean for anthropogenic CO_2.

The global coastal margin will likely remain in a state of heterotrophy because its organic balance is strongly influenced by land-use activities (fig. 7). These activities generally increase riverine discharge of organic matter to the coastal margin. Studies have shown that the rate of delivery of carbon and nutrients from the terrestrial reservoirs to the coastal zone, including those from the loading of human sewage and municipal wastewater, is closely correlated to human activities on land (Cole and others, 1993; Caraco, 1995). In the Chiang Jiang River (Yangtze River) in China for example, the oxidative consumption of organic matter transported from land can be a significant source of P in its estuaries and the coastal waters of the East China Sea (Rao and Berner, 1994). A similar conclusion, that coastal zone metabolism is controlled by the delivery of terrestrial organic matter via rivers, rather than by changes in temperature, was derived from process-based studies reported by Smith and Hollibaugh (1993).

Further analysis of our results suggests that were it not for the supply of dissolved and particulate carbon from soil degradation and water runoff to the coastal zone, the continued application of inorganic fertilizers on land would eventually have caused the coastal zone to become net autotrophic, hence a net sink for CO_2 involved in organic metabolism. This result is in agreement with observations that regional-scale coastal

environments with primarily inorganic nutrient inputs tend to develop into a more autotrophic state (Smith and Mackenzie, 1987; Smith and Hollibaugh, 1993). Thus the future state of the organic carbon balance or the net ecosystem metabolism of the global coastal zone will depend to a considerable extent on the changes in magnitude of the flux of organic matter relative to that of inorganic nutrients to coastal environments. Both these fluxes are significantly affected by human activities.

It has been shown, using the same model analysis (Ver, Mackenzie, and Lerman, 1999), that the direction of net transfer of CO_2 between the atmosphere and coastal ocean can be strongly affected by changes in the global thermohaline circulation of the ocean on time scales of several decades to a century. At present, upwelling of deep ocean water, enriched in dissolved inorganic carbon (DIC), as well as inorganic nutrients N and P, supplies much of these elements to the coastal zone. The upwelled DIC, together with the DIC produced by calcium-carbonate deposition and mineralization of organic matter, counteracts the flux of CO_2 from the atmosphere to the coastal ocean. Reduction or cessation of the present pattern of the thermohaline circulation of the ocean would reduce the supply of DIC to the coastal zone, thereby possibly making it a more effective sink for anthropogenic CO_2 in the atmosphere.

VI. CO_2 EMISSION STRATEGIES AND FUTURE ATMOSPHERIC CO_2 CONCENTRATIONS

In recent years, much attention has been devoted to the future accumulation of CO_2 in the atmosphere and its climatic consequences. Projections made by the Intergovernmental Panel on Climate Change (IPCC) are those most commonly cited (Houghton and others, 1996). Here we make some future projections for atmospheric CO_2 concentrations using TOTEM. As in any model-based projections, ours can be used only as guidelines to the behavior of the global carbon cycle in the future under sustained perturbations by human activities.

For our analysis of the carbon cycle in the near future, we chose two fossil-fuel emission scenarios: the "business as usual" (BAU) IS92a scenario of the IPCC (Houghton and others, 1996) and the Kyoto Protocol of the 1997 United Nations Framework Convention on Climate Change (UNFCCC). The Kyoto Protocol sets international guidelines for a collective reduction by 39 developed countries of their aggregate anthropogenic emissions of greenhouse gases (in terms of CO_2 equivalent emissions) to 5.2 percent below 1990 levels during the period 2008 to 2012. Each participating country has chosen its own target within this framework – for example, the United States would reduce emissions to 7 percent below the 1990 level within the prescribed period.

We computed future atmospheric CO_2 concentrations for several decades into the 21st century, using the BAU and the Kyoto Protocol fossil fuel emission scenarios in our model TOTEM, and compared these results to the IPCC future CO_2 concentration estimates up to the year 2075. For the Kyoto Protocol scenario, we assume that global CO_2 emissions from fossil fuel burning will decrease linearly during the years 2001 to 2012, with emissions effectively reduced and maintained at 5 percent below their 1990 level after the year 2012, at approx 5.8 Gt C/yr. The effect of emission reductions on other greenhouse gases, such as methane, nitrous oxide, and chlorofluorocarbons, was not considered in this analysis.

The fossil fuel emissions (from both BAU IS92a and Kyoto Protocol projected estimates) are only one of the five forcings used in TOTEM. The other four projected forcing functions for the period 1996 to 2075 are the same for both experiments. Global temperature projections are from the IPCC (Houghton and others, 1996); land-use change, agricultural fertilizer inputs, and sewage discharges are based on population and agricultural statistical projections by various agencies of the UN (United Nations Population Division, 1995; United Nations FAO, various years).

Figure 6B shows a comparison of the projections for global mean atmospheric CO_2 concentrations computed using TOTEM and the IPCC projection for the BAU IS92a scenario. The TOTEM results for the BAU emissions are in general agreement with the

IPCC projection, but the differences are important. TOTEM projects for the early and middle 21st century slightly higher atmospheric CO_2 levels (550 ppmv) than those of the IPCC model (510 ppmv). This difference reflects mainly the following: differences in the future land-use scenarios of the two models; the fact that the IPCC model uses a constant CO_2 fertilization factor; and in TOTEM, the model processes depend on interactions between environmental variables and temperature, some of which are non-linear functions (see sect. IIA).

For the model conditions approximating those of the Kyoto Protocol, the results show that by the year 2010, the global mean atmospheric CO_2 concentration will have risen by about 20 ppmv, despite a cumulative reduction of 15 percent in fossil fuel emissions relative to that of the year 2000. In comparison, atmospheric CO_2 will increase by about 25 ppmv under the less restrictive BAU emissions, with a 20 percent increase in emissions relative to that of the year 2000. The somewhat sluggish response by the atmospheric CO_2 reservoir to the case of the reduced emissions may be attributed to the continued rise in CO_2 emissions from land-use changes and the 10-yr mean residence time of CO_2 in the atmosphere. The effect of reductions in the fossil fuel emissions on atmospheric CO_2 concentrations becomes progressively more evident over a longer period toward mid-century. By the year 2050, fossil fuel emissions under the more stringent terms of the Kyoto Protocol would amount to only 40 percent of the BAU emissions. By that time, the global mean atmospheric CO_2 concentration from TOTEM analysis is projected to be 90 ppmv less than the concentration based on BAU emissions (about 460 versus 550 ppmv) and 40 ppmv less than the IPCC projection for the case of BAU emissions (about 460 versus 510 ppmv).

It may be anticipated that this reduction in the rate of accumulation of atmospheric CO_2 would be maintained unless other mechanisms were to increase or decrease the drawdown of CO_2. Such mechanisms could be, for example, feedback through fertilization of the land phytomass and enhanced photosynthetic production or, in the opposite direction, enhanced respiration of organic matter on land or reduction in the intensity of the ocean thermohaline circulation. It appears, therefore, that the 1997 UN Kyoto Protocol, setting emission limits for greenhouse gases, may be a mechanism for stemming the increase in atmospheric CO_2, but only if the physical and biogeochemical mechanisms of redistribution of CO_2 among the atmosphere, land, and ocean do not significantly change from the present.

VII. CONCLUSIONS

With the process-driven model of the coupled C-N-P-S global cycles (TOTEM), we were able to model very closely the historical rise in atmospheric CO_2 concentrations during the past 300 yrs and the partitioning of anthropogenic CO_2 emissions among the biogeochemical sinks of the atmosphere, land, coastal ocean, and open ocean. It appears that the magnitude and maintenance of any CO_2 fertilization effect on the terrestrial biosphere are primarily due to nutrients (N and P) in organic matter that are remobilized and translocated during land-use activities. These activities also enhance the source fluxes of CO_2 to the atmosphere. Thus changes in land-use activities may potentially either reduce or amplify the sink strength associated with the CO_2 fertilization effect. For example, worldwide decrease in the magnitude of land-use activities, resulting in smaller amounts of nutrient N and P releases from the recycling of organic matter and the strong possibility of continuously rising mean global temperature that increases the rates of terrestrial gross respiration (Woodwell and Mackenzie, 1995; Woodwell and others, 1998) might conceivably lead to a considerable weakening of the inferred terrestrial sink of anthropogenic CO_2.

Environmental changes on land are rapidly conveyed downstream to the coastal zone, which is not a surprising conclusion of the model analysis because of the relatively short residence times of fresh water on land. The residence time of river water is of the order of only 20 days with respect to net rainfall over land or to continental runoff. Thus,

any reconfiguration of agricultural and industrial practices on land has the potential to affect downcycle reservoirs, such as continental soilwater, groundwaters, lakes, and the coastal ocean, on the decadal to century time scale. Of particular interest is the fact that if terrestrial ecosystems have been undergoing fertilization by anthropogenic CO_2, N, and P, then we would expect changes in the cycling of inorganic and organic carbon in the coastal zone (or, from an ecological perspective, changes in organic metabolism of coastal ecosystems), downstream from the regions affected by fertilization processes, with significant implications for the magnitude and direction of the net exchange flux of CO_2 gas across the air-seawater interface. If terrestrial fertilization were the only process affecting organic metabolism in coastal ecosystems, we would anticipate a global trend toward increasing heterotrophy of such systems during the 21st century (increasing excess of organic carbon oxidized over the amount fixed by photosynthesis).

Finally, our analysis of future atmospheric CO_2 concentrations of the 21st century, based on two sets of projections of fossil fuel emissions (IPCC BAU and the UNFCCC Kyoto Protocol), shows that the rate of atmospheric CO_2 growth in the future strongly depends on the reduction of CO_2 emissions from fossil fuel combustion. In addition, the analysis demonstrates that N and P inputs to terrestrial ecosystems and feedback mechanisms to the storage or release of carbon by the terrestrial organic reservoirs are critical factors that must be considered in projecting future atmospheric CO_2 concentrations. Any policy designed to control future atmospheric CO_2 concentration levels must include consideration of the whole Earth system, including the nonlinear behavior of processes and feedback mechanisms affecting C, N, P, and S in the land, atmosphere, coastal ocean, and open ocean domains.

ACKNOWLEDGMENTS

This research was supported by National Science Foundation Grant EAR93-16133 and by NOAA Office of Global Programs Grant NA37RJ0199. We thank Gabriel Filippelli (Indiana-Purdue University), Robert Berner (Yale University), James Galloway (University of Virginia), Patrick Holligan (Southampton Oceanography Center), and Telu Li, Christopher Measures, Brian Popp, Jane Tribble, and Steven V. Smith (University of Hawaii) for their critical comments on various parts of this paper. During writing of a preliminary draft of the manuscript, FTM and AL were Fellows at the Wissenschaftskolleg zu Berlin, and we thank the Institute and its Rector, Professor Dr. Wolf Lepenies, for providing the space and atmosphere for unbridled thinking. School of Ocean and Earth Science and Technology Contribution No. 4852. Correspondence and requests for materials should be addressed to FTM: fredm@goldschmidt.soest.hawaii.edu

Appendix A

Numerical or letter subscripts denote each of the 13 reservoirs and the rivers and streams (fig. 1, table 1A). The term C_1, for example, is the mass of carbon in terrestrial phytomass. In the flux term XF_{ij}, X = C (carbon), N (nitrogen), P (phosphorus), or S (sulfur); the subscripts i = originating reservoir, and j = receiving reservoir. Net exchange fluxes of carbon between the atmosphere and surface waters and between the surface and deep ocean are indicated as CF_{iji} (for example, CF_{4104}, CF_{7107}, CF_{797}). Other subscripts used are: atmex = exchange between the atmosphere and surface waters; Detergent = detergent consumption; diss = dissolved; Fert = inorganic fertilizers; Fert cons = fertilizer consumption; FF = fossil fuel and cement manufacturing; hydro = hydrothermal; inorg = inorganic; LU = land-use; org = organic; out = outside of defined model boundaries (that is, external); part = particulate; photo = photosynthesis; react = reactive; resp = respiration; Sewage = sewage discharge; unr = unreactive; and Redfield ratios are defined in section IIIE and denoted in the equations as, for example, $(C:P)_{1\ photo}$. Reservoir masses are in units of 10^{12} moles of the element; fluxes are in units of 10^{12} moles of element/yr; rate constants are in units of 1/yr.

I. EQUATIONS OF THE MODEL TOTEM

IA. Carbon Equations

IA1. Mass balance equations

$$C_1(t) = C_1(t - dt) + (CF_{101} - CF_{12} - CF_{110} - CF_{1LU}) \times dt$$

$C_2(t) = C_2(t - dt) + (CF_{12} + CF_{out2} - CF_{2Sw} - CF_{2LU} - CF_{2R}) \times dt$
$C_3(t) = C_3(t - dt) + (CF_{out3} - CF_{3Sw} - CF_{3R}) \times dt$
$C_4(t) = C_4(t - dt) + (CF_{54} + CF_{64\ inorg} + CF_{64\ org} + CF_{94} + CF_{R4} + CF_{4104} - CF_{45} - CF_{46} - CF_{47}) \times dt$
$C_5(t) = C_5(t - dt) + (CF_{45} + CF_{R5\ diss} + CF_{R5\ part} + CF_{Sewage} - CF_{54} - CF_{56} - CF_{58}) \times dt$
$C_6(t) = C_6(t - dt) + (CF_{46} + CF_{56} + CF_{R6\ org} + CF_{R6\ inorg} - CF_{64\ inorg} - CF_{64\ org} - CF_{6out\ org} - CF_{6out\ inorg} - CF_{69}) \times dt$
$C_7(t) = C_7(t - dt) + (CF_{47} + CF_{7107} + CF_{87} - CF_{78} - CF_{797}) \times dt$
$C_8(t) = C_8(t - dt) + (CF_{58} + CF_{78} - CF_{87} - CF_{89}) \times dt$
$C_9(t) = C_9(t - dt) + (CF_{69} + CF_{797} + CF_{89} + CF_{hydro} - CF_{94} - CF_{9out\ org} - CF_{9out\ inorg}) \times dt$
$C_{10}(t) = C_{10}(t - dt) + CF_{110} + CF_{out10} + CF_{Sw10} + CF_{1LU} + CF_{2LU} + C_{FF} - CF_{101} - CF_{4104} - CF_{7107}) \times dt$
$C_{Gw}(t) = C_{Gw}(t - dt) + (CF_{SwGw} - CF_{GwR}) \times dt$
$C_{La}(t) = C_{La}(t - dt) + (CF_{SwLa} - CF_{LaR}) \times dt$
$C_R(t) = C_R(t - dt) + (CF_{SwR} + CF_{GwR} + CF_{2R} + CF_{3R} + CF_{LaR} - CF_{R4} - CF_{R5\ diss} - CF_{R5\ part} - CF_{R6\ org} - CF_{R6\ inorg}) \times dt$
$C_{Sw}(t) = C_{Sw}(t - dt) + (CF_{2Sw} + CF_{3Sw} - CF_{Sw10} - CF_{SwR} - CF_{SwGw} - CF_{SwLa}) \times dt$

IA2. Flux equations

$CF_{12} = kC_{12} \times C_1(t)$ $CF_{110} = kC_{110} \times C_1(t) \times f_T$ $CF_{1LU} = f_{LU} \times C_{LU}$
$CF_{2Sw} = kC_{2Sw} \times C_2(t) \times f_T$ $CF_{2LU} = (1 - f_{LU}) \times C_{LU}$ $CF_{2R} = CF_{2R\ t=0} \times (1 + f_{LUR})$
$CF_{3Sw} = kC_{3Sw} \times C_3(t)$ $CF_{3R} = CF_{3R\ t=0} \times (1 + f_{LUR})$
$CF_{45} = CF_{45\ t=0} \times f_{N4} \times f_{P4}$ $CF_{46} = kC_{46} \times C_4(t)$ $CF_{47} = kC_{47} \times C_4(t)$
$CF_{54} = kC_{54} \times C_5(t)$ $CF_{56} = kC_{56} \times C_5(t)$ $CF_{58} = kC_{58} \times C_5(t)$
$CF_{64\ org} = kC_{64\ org} \times C_6(t)$ $CF_{64\ inorg} = kC_{64\ inorg} \times C_6(t)$ $CF_{69} = kC_{69} \times C_6(t)$
$CF_{6out\ org} = 9$ $CF_{6out\ inorg} = kC_{6out\ inorg} \times C_6(t)$
$CF_{78} = CF_{78\ t=0} \times f_{N7} \times f_{P7}$
$CF_{797} = -CF_{797\ t=0} + [(C_7(t) - C_{7\ t=0})/(h_7 \times \tau_9)] - [C_9(t) - C_{9\ t=0})/(h_9 \times \tau_9)]$
$CF_{87} = kC_{87} \times C_8(t)$ $CF_{89} = kC_{89} \times C_8(t)$
$CF_{94} = kC_{94} \times C_9(t)$ $CF_{9out\ inorg} = kC_{9out\ inorg} \times C_9(t)$ $CF_{9out\ org} = 2$
$CF_{101} = kC_{101} \times C_1(t) \times K_{photo} = GPP$
$CF_{4104} = (dC_4/dt)_{atmex} - \{CF_{R4} + CF_{54} + CF_{64\ org} + CF_{64\ inorg} + CF_{94} - CF_{45} - CF_{46} - CF_{47}\}$
$CF_{7107} = (dC_7/dt)_{atmex} - \{CF_{47} + CF_{87} - CF_{78} - CF_{797}\}$
$CF_{GwR} = kC_{GwR} \times C_{Gw}(t)$
$CF_{LaR} = kC_{LaR} \times C_{La}(t)$
$CF_{R4} = kC_{R4} \times C_R(t)$ $CF_{R5\ diss} = kC_{R5\ diss} \times C_R(t)$ $CF_{R5\ part} = kC_{R5\ part} \times C_R(t)$
$CF_{R6\ org} = kC_{R6\ org} \times C_R(t)$ $CF_{R6\ inorg} = kC_{R6\ inorg} \times C_R(t)$
$CF_{Sw10} = kC_{Sw10} \times C_{Sw}(t) \times f_T$ $CF_{SwR} = kC_{SwR} \times C_{Sw}(t)$ $CF_{SwGw} = kC_{SwGw} \times C_{Sw}(t)$
$CF_{SwLa} = kC_{SwLa} \times C_{Sw}(t)$
$CF_{out2} = 5$ $CF_{out3} = 26$ $CF_{hydro} = 5$
$CF_{out10} = 8$

IB. Nitrogen Equations

IB1. Mass balance equations

$N_1(t) = N_1(t - dt) + (NF_{Sw1} + NF_{101} - NF_{12} - NF_{1LU}) \times dt$
$N_2(t) = N_2(t - dt) + (NF_{12} - NF_{2Sw} - NF_{2LU} - NF_{2R}) \times dt$
$N_3(t) = N_3(t - dt) + (NF_{out3} - NF_{3Sw} - NF_{3R}) \times dt$
$N_4(t) = N_4(t - dt) + (NF_{54} + NF_{64} + NF_{94} + NF_{104} + N_{FF4} + NF_{R4} - NF_{45} - NF_{47} - NF_{410}) \times dt$
$N_5(t) = N_5(t - dt) + (NF_{45} + NF_{105} + NF_{R5\ diss} + NF_{R5\ part} + NF_{Sewage} - NF_{54} - NF_{56} - NF_{58}) \times dt$
$N_6(t) = N_6(t - dt) + (NF_{56} + NF_{R6\ org} + NF_{R6\ inorg} - NF_{64} - NF_{6out} - NF_{610}) \times dt$
$N_7(t) = N_7(t - dt) + (NF_{47} + NF_{87} + NF_{97} + NF_{107} - NF_{78} - NF_{79} - NF_{710}) \times dt$
$N_8(t) = N_8(t - dt) + (NF_{58} + NF_{78} + NF_{108} - NF_{87} - NF_{89}) \times dt$
$N_9(t) = N_9(t - dt) + (NF_{79} + NF_{89} - NF_{94} - NF_{97} - NF_{9out}) \times dt$
$N_{10}(t) = N_{10}(t - dt) + (NF_{410} + NF_{610} + NF_{710} + NF_{Sw10} - NF_{101} - NF_{104} - NF_{105} - NF_{107} - NF_{108} - NF_{10Sw}) \times dt$
$N_{Gw}(t) = N_{Gw}(t - dt) + (NF_{SwGw} - NF_{GwR}) \times dt$
$N_{La}(t) = N_{La}(t - dt) + (NF_{SwLa} - NF_{LaR}) \times dt$
$N_R(t) = N_R(t - dt) + (NF_{LaR} + NF_{GwR} + NF_{FertR} + NF_{SwR} + NF_{2R} + NF_{3R} - NF_{R4} - NF_{R5\ diss} - NF_{R5\ part} - NF_{R6\ org} - NF_{R6\ inorg}) \times dt$
$N_{Sw}(t) = N_{Sw}(t - dt) + (NF_{2Sw} + NF_{3Sw} + NF_{10Sw} + NF_{1LU} + NF_{2LU} + N_{FFSw} + NF_{Fert\ leach} - NF_{Sw1} - NF_{Sw10} - NF_{SwGw} - NF_{SwLa} - NF_{SwR}) \times dt$

IB2. Flux equations

$NF_{12} = kN_{12} \times N_2(t)$
$NF_{1LU} = CF_{1LU}/(C:N)_{1\ resp}$
$NF_{2Sw} = kN_{2Sw} \times N_2(t) \times f_T$
$NF_{2LU} = CF_{2LU}/(C:N)_{2\ resp}$
$NF_{2R} = NF_{2R\ t=0} \times (1 + f_{LUR})$
$NF_{3Sw} = kN_{3Sw} \times N_3(t)$
$NF_{3R} = NF_{3R\ t=0} \times (1 + f_{LUR})$
$NF_{45} = CF_{45}/(C:N)_{5\ photo}$
$NF_{47} = kN_{47} \times N_4(t)$
$NF_{410} = kN_{410} \times N_4(t)$
$NF_{54} = kN_{54} \times N_5(t)$
$NF_{56} = kN_{56} \times N_5(t)$
$NF_{58} = kN_{58} \times N_5(t)$
$NF_{64} = kN_{64} \times N_6(t)$
$NF_{610} = kN_{610} \times N_6(t)$
$NF_{6out} = 0.22$
$NF_{78} = CF_{78}/(C:N)_{8\ photo}$
$NF_{79} = kN_{79} \times N_7(t)$
$NF_{710} = kN_{710} \times N_7(t)$
$NF_{87} = kN_{87} \times N_8(t)$
$NF_{89} = kN_{89} \times N_8(t)$
$NF_{94} = kN_{94} \times N_9(t)$
$NF_{97} = kN_{97} \times N_9(t)$
$NF_{9out} = 0.08$
$NF_{101} = 9.0$
$NF_{104} = kN_{104} \times N_{10}(t)$
$NF_{105} = 2.37$
$NF_{107} = kN_{107} \times N_{10}(t)$
$NF_{108} = 0.63$
$NF_{10Sw} = kN_{10Sw} \times N_{10}(t)$
$NF_{GwR} = kN_{GwR}(t) \times N_{Gw}(t)$
$NF_{LaR} = kN_{LaR}(t) \times N_{La}(t)$
$NF_{R4} = kN_{R4} \times N_R(t)$
$NF_{R5\ diss} = kN_{R5\ diss} \times N_R(t)$
$NF_{R5\ part} = kN_{R5\ part} \times N_R(t)$
$NF_{R6\ org} = kN_{R6\ org} \times N_R(t)$
$NF_{R6\ inorg} = kN_{R6\ inorg} \times N_R(t)$
$NF_{Sw1} = CF_{101}/(C:N)_{1\ photo}$
$NF_{Sw10} = kN_{Sw10} \times N_{Sw}(t) \times f_T$
$NF_{SwGw} = kN_{SwGw} \times N_{Sw}(t)$
$NF_{SwLa} = kN_{SwLa} \times N_{Sw}(t)$
$NF_{SwR} = kN_{SwR} \times N_{Sw}(t)$
$NF_{out3} = 0.30$

IC. Phosphorus Equations

IC1. Mass balance equations

$P_1(t) = P_1(t - dt) + (PF_{Sw1} - PF_{12} - PF_{1LU} - PF_{1LU\ unr}) \times dt$
$P_2(t) = P_2(t - dt) + (PF_{12} - PF_{2Sw} - PF_{2LU} - PF_{2LU\ unr} - PF_{2R}) \times dt$
$P_3(t) = P_3(t - dt) + (PF_{out3} + PF_{1LU\ unr} + PF_{2LU\ unr} + PF_{Fert\ unr} - PF_{3Sw} - PF_{3R}) \times dt$
$P_4(t) = P_4(t - dt) + (PF_{54} + PF_{64} + PF_{94} + PF_{R4} + PF_{Detergent} - PF_{45} - PF_{47}) \times dt$
$P_5(t) = P_5(t - dt) + (PF_{45} + PF_{R5\ diss} + PF_{R5\ part} + PF_{Sewage} - PF_{54} - PF_{56} - PF_{58}) \times dt$
$P_6(t) = P_6(t - dt) + (PF_{56} + PF_{R6\ org} + PF_{R6\ inorg} - PF_{64} - PF_{6out}) \times dt$
$P_7(t) = P_7(t - dt) + (PF_{47} + PF_{87} + PF_{97} - PF_{78} - PF_{79}) \times dt$
$P_8(t) = P_8(t - dt) + (PF_{58} + PF_{78} - PF_{87} - PF_{89}) \times dt$
$P_9(t) = P_9(t - dt) + (PF_{79} + PF_{89} - PF_{94} - PF_{97} - PF_{9out}) \times dt$
$P_{Gw}(t) = P_{Gw}(t - dt) + (PF_{SwGw} - PF_{GwR}) \times dt$
$P_{La}(t) = P_{La}(t - dt) + (PF_{SwLa} - PF_{LaR}) \times dt$
$P_R(t) = P_R(t - dt) + (PF_{SwR} + PF_{GwR} + PF_{LaR} + PF_{FertR} + PF_{2R} + PF_{3R} - PF_{R4} - PF_{R5\ diss} - PF_{R5\ part} - PF_{R6\ org} - PF_{R6\ inorg}) \times dt$
$P_{Sw}(t) = P_{Sw}(t - dt) + (PF_{2Sw} + PF_{3Sw} + PF_{1LU} + PF_{2LU} + PF_{Fert\ leach} - PF_{Sw1} - PF_{SwGw} - PF_{SwLa} - PF_{SwR}) \times dt$

IC2. Flux equations

$PF_{12} = kP_{12} \times P_1(t)$
$PF_{1LU} = CF_{1LU} \times fP_{LU\ react}/(C:P)_{1\ resp}$
$PF_{1LU\ unr} = CF_{1LU} \times (1 - fP_{LU\ react})/(C:P)_{1\ resp}$
$PF_{2Sw} = kP_{2Sw} \times P_2(t) \times f_T$
$PF_{2LU} = CF_{2LU} \times fP_{LU\ react}/(C:P)_{2\ resp}$
$PF_{2R} = PF_{2R\ t=0} \times (1 + f_{LUR})$
$PF_{2LU\ unr} = CF_{2LU} \times (1 - fP_{LU\ react})/(C:P)_{2\ resp}$
$PF_{3Sw} = kP_{3Sw} \times P_3(t) \times f_T$
$PF_{3R} = PF_{3R\ t=0} \times (1 + f_{LUR}) \times f_T$
$PF_{45} = CF_{45}/(C:P)_{5\ photo}$
$PF_{47} = kP_{47} \times P_4(t)$
$PF_{54} = kP_{54} \times P_5(t)$
$PF_{56} = kF_{56} \times P_5(t)$
$PF_{58} = kP_{58} \times P_5(t)$
$PF_{64} = kP_{64} \times P_6(t)$
$PF_{6out} = 0.59$
$PF_{78} = CF_{78}/(C:P)_{8\ photo}$
$PF_{79} = kP_{79} \times P_7(t)$
$PF_{87} = kP_{87} \times P_8(t)$
$PF_{89} = kP_{89} \times P_8(t)$
$PF_{94} = kP_{94} \times P_9(t)$
$PF_{97} = kP_{97} \times P_9(t)$
$PF_{9out} = 0.089$
$PF_{GwR} = kP_{GwR} \times P_{Gw}(t)$
$PF_{LaR} = kP_{LaR} \times P_{La}(t)$
$PF_{R4} = kP_{R4} \times P_R(t)$
$PF_{R5\ diss} = kP_{R5\ diss} \times P_R(t)$
$PF_{R5\ part} = kP_{R5\ part} \times P_R(t)$
$PF_{R6\ org} = kP_{R6\ org} \times P_R(t)$
$PF_{R6\ inorg} = kP_{R6\ inorg} \times P_R(t)$
$PF_{Sw1} = CF_{101}/(C:P)_{1\ photo}$
$PF_{SwGw} = kP_{SwGw} \times P_{Sw}(t)$
$PF_{SwLa} = kP_{SwLa} \times P_{Sw}(t)$
$PF_{SwR} = kP_{SwR} \times P_{Sw}(t)$
$PF_{out3} = 0.677$

ID. Sulfur Equations

ID1. Mass balance equations

$S_1(t) = S_1(t - dt) + (SF_{Sw1} - SF_{12} - SF_{110} - SF_{1LU}) \times dt$

$S_2(t) = S_2(t - dt) + (SF_{12} - S_{2LU} - SF_{2R} - SF_{2Sw}) \times dt$

$S_3(t) = S_3(t - dt) + (SF_{out3} - SF_{310} - SF_{3R} - SF_{3Sw}) \times dt$

$S_4(t) = S_4(t - dt) + (SF_{54} + SF_{64} + SF_{94} + SF_{104} + SF_{R4} + S_{FF4} - SF_{45} - SF_{47} - SF_{410}) \times dt$

$S_5(t) = S_5(t - dt) + (SF_{45} + SF_{R5\,diss} + SF_{R5\,part} - SF_{54} - SF_{56} - SF_{58} - SF_{510}) \times dt$

$S_6(t) = S_6(t - dt) + (SF_{56} + SF_{R6\,inorg} + SF_{R6\,org} - SF_{64} - SF_{6out}) \times dt$

$S_7(t) = S_7(t - dt) + (SF_{47} + SF_{87} + SF_{107} - SF_{78} - SF_{710}) \times dt$

$S_8(t) = S_8(t - dt) + (SF_{58} + SF_{78} - SF_{87} - SF_{89}) \times dt$

$S_9(t) = S_9(t - dt) + (SF_{89} + SF_{hydro} - SF_{94} - SF_{9out}) \times dt$

$S_{10}(t) = S_{10}(t - dt) + (SF_{110} + SF_{310} + SF_{410} + SF_{510} + SF_{710} + SF_{Sw10} + SF_{out10} - SF_{104} - SF_{107} - SF_{10Sw}) \times dt$

$S_{Gw}(t) = S_{Gw}(t - dt) + (SF_{SwGw} - SF_{GwR}) \times dt$

$S_{La}(t) = S_{La}(t - dt) + (SF_{SwLa} - SF_{LaR}) \times dt$

$S_R(t) = S_R(t - dt) + (SF_{2R} + SF_{3R} + SF_{GwR} + SF_{LaR} + SF_{SwR} - SF_{R4} - SF_{R5\,diss} - SF_{R5\,part} - SF_{R6\,inorg} - SF_{R6\,org}) \times dt$

$S_{Sw}(t) = S_{Sw}(t - dt) + (SF_{1LU} + SF_{2LU} + SF_{2Sw} + SF_{3Sw} + SF_{10Sw} + S_{FFSw} - SF_{Sw1} - SF_{Sw10} - SF_{SwGw} - SF_{SwLa} - SF_{SwR}) \times dt$

ID2. Flux equations

$SF_{12} = kS_{12} \times S_1(t)$	$SF_{110} = kS_{110} \times S_1(t)$	$SF_{1LU} = CF_{1LU}/(C{:}S)_{1\,resp}$
$SF_{2LU} = CF_{2LU}/(C{:}S)_{2\,resp}$	$SF_{2R} = SF_{2R\,t=0} \times (1 + f_{LUR})$	$SF_{2Sw} = kS_{2Sw} \times S_2(t) \times f_T$
$SF_{310} = kS_{310} \times S_3(t)$	$SF_{3R} = SF_{3R\,t=0} \times (1 + f_{LUR})$	$SF_{3Sw} = kS_{3Sw} \times S_3(t)$
$SF_{45} = CF_{45}/(C{:}S)_{5\,photo}$	$SF_{47} = kS_{47} \times S_4(t)$	$SF_{410} = kS_{410} \times S_4(t)$
$SF_{54} = kS_{54} \times S_5(t)$	$SF_{56} = kS_{56} \times S_5(t)$	$SF_{58} = kS_{58} \times S_5(t)$
$SF_{510} = kS_{510} \times S_5(t)$		
$SF_{64} = kS_{64} \times S_6(t)$	$SF_{6out} = 0.982$	
$SF_{78} = CF_{78}/(C{:}S)_{8\,photo}$	$SF_{710} = kS_{710} \times S_7(t)$	
$SF_{87} = kS_{87} \times S_8(t)$	$SF_{89} = kS_{89} \times S_8(t)$	
$SF_{94} = kS_{94} \times S_9(t)$	$SF_{9out} = 0.218$	
$SF_{104} = kS_{104} \times S_{10\,Input}$	$SF_{107} = kS_{107} \times S_{10\,Input}$	$SF_{10Sw} = kS_{10Sw} \times S_{10\,Input}$
$S_{10\,Input} = SF_{110} + SF_{310} + SF_{410} + SF_{510} + SF_{710} + SF_{Sw10} + SF_{out10}$		
$SF_{GwR} = kS_{GwR} \times S_{Gw}(t)$		
$SF_{LaR} = kS_{LaR} \times S_{La}(t)$		
$SF_{R4} = kS_{R4} \times S_R(t)$	$SF_{R5\,diss} = kS_{R5\,diss} \times S_R(t)$	$SF_{R5\,part} = kS_{R5\,part} \times S_R(t)$
$SF_{R6\,inorg} = kS_{R6\,inorg} \times S_R(t)$	$SF_{R6\,org} = kS_{R6\,org} \times S_R(t)$	
$SF_{Sw1} = CF_{101}/(C{:}S)_{1\,photo}$	$SF_{Sw10} = kS_{Sw10} \times S_{Sw}(t) \times f_T$	$SF_{SwGw} = kS_{SwGw} \times S_{Sw}(t)$
$SF_{SwLa} = kS_{SwLa} \times S_{Sw}(t)$	$SF_{SwR} = kS_{SwR} \times S_{Sw}(t)$	
$SF_{out3} = 1.124$	$SF_{hydro} = 0.013$	$SF_{out10} = 0.063$

II. ANTHROPOGENIC FLUXES

IIA. Fossil Fuel Burning

C_{FF} = total CO_2 emissions from fossil fuel burning and cement manufacturing (Marland and others, 1998)

$N_{FF4} = N_{FF} \times fN_{FF4}$

$N_{FFSw} = N_{FF} \times (1 - fN_{FF4})$

$N_{FF} = N_{FF4} + N_{FFSw}$; total anthropogenic NO_x emissions (Dignon and Hameed, 1989; Dignon, 1992; Hameed and Dignon, 1992; Brown, Renner, and Flavin, 1997)

$fN_{FF4} = 0.379$; fraction of NO_x emissions that is deposited back onto the coastal water reservoir

$S_{FF4} = S_{FF} \times fS_{FF4}$

$S_{FFSw} = S_{FF} \times (1 - fS_{FF4})$

$S_{FF} = S_{FF4} + SN_{FFSw}$; total anthropogenic SO_x emissions (Dignon and Hameed, 1989; Dignon, 1992; Hameed and Dignon, 1992; Brown, Renner, and Flavin, 1997)

$fS_{FF4} = 0.5$; fraction of SO_x emissions that is deposited back onto the coastal water reservoir

IIB. Changes in Land-Use Activities

$CF_{1LU} = f_{LU} \times C_{LU}$; emissions of CO_2 from land-use disturbance of terrestrial biota
$CF_{2LU} = (1 - f_{LU}) \times C_{LU}$; emissions of CO_2 from land-use disturbance of humus
$NF_{1LU} = CF_{1LU}/(C{:}N)_{1\ resp}$
$NF_{2LU} = CF_{2LU}/(C{:}N)_{2\ resp}$
$PF_{1LU} = CF_{1LU} \times fP_{LU\ react}/(C{:}P)_{1\ resp}$
$PF_{1LU\ unr} = CF_{1LU} \times (1 - fP_{LU\ react})/(C{:}P)_{1\ resp}$
$PF_{2LU} = CF_{2LU} \times fP_{LU\ react}/(C{:}P)_{2\ resp}$
$PF_{2LU\ unr} = CF_{2LU} \times (1 - fP_{LU\ react})/(C{:}P)_{2\ resp}$
$SF_{1LU} = CF_{1LU}/(C{:}S)_{1\ resp}$
$SF_{2LU} = CF_{2LU}/(C{:}S)_{1\ resp}$
$C_{LU} = C_{1LU} + C_{2LU}$; total CO_2 emissions from land-use activities (Houghton, 1983; Houghton, 1991b; Houghton, 1991a; Kammen and Marino, 1993)
$f_{LU} = 0.25$; fraction of land-use CO_2 emissions from terrestrial biota
$fP_{LU\ react} = 0.7$; $1700 < t < 1930$
$= 1.0$; $t > 1930$; fraction of remobilized P that remains in the reactive inorganic form
$CF_{2R} = CF_{2R\ t=0} \times (1 + f_{LUR})$
$CF_{3R} = CF_{3R\ t=0} \times (1 + f_{LUR})$
$NF_{2R} = NF_{2R\ t=0} \times (1 + f_{LUR})$
$NF_{3R} = NF_{3R\ t=0} \times (1 + f_{LUR})$
$PF_{2R} = PF_{2R\ t=0} \times (1 + f_{LUR})$
$PF_{3R} = PF_{3R\ t=0} \times (1 + f_{LUR}) \times f_T$
$SF_{2R} = SF_{2R\ t=0} \times (1 + f_{LUR})$
$SF_{3R} = SF_{3R\ t=0} \times (1 + f_{LUR})$
$f_{LUR} = 0.008 \times (C_{LU} - C_{LU\ t=0})$; effect of land-use activities on the transport of C, N, P, and S to coastal margins via runoff.

IIC. Agricultural Fertilizer Application

$NF_{Fert\ crops} = NF_{Fert\ cons} \times fN_{Fert\ crops}$; applied N fertilizer that is assimilated into crops
$NF_{Fert\ leach} = NF_{Fert\ cons} \times fNP_{Fert\ leach}$; applied N fertilizer that leaches into soil water reservoir
$NF_{FertR} = NF_{Fert\ cons} \times fN_{FertR}$; applied N fertilizer that is lost in runoff
$NF_{FertVol} = NF_{Fert\ cons} - NF_{Fert\ crops} - NF_{Fert\ leach} - NF_{FertR}$; applied N fertilizer that is volatilized
$PF_{Fert\ crops} = NF_{Fert\ crops}/(N{:}P)_{Crops}$; applied P fertilizer that is assimilated into crops
$PF_{Fert\ leach} = PF_{Fert\ cons} \times fNP_{Fert\ leach}$; applied P fertilizer that leaches into soilwater reservoir
$PF_{FertR} = PF_{Fert\ cons} \times fP_{FertR}$; applied P fertilizer that is lost in runoff
$PF_{Fert\ unr} = PF_{Fert\ cons} - PF_{Fert\ crops} - PF_{Fert\ leach} - PF_{FertR}$; applied P fertilizer that is transformed into the biochemically unreactive inorganic form
$NF_{Fert\ cons} = NF_{Fert\ crops} + NF_{Fert\ leach} + NF_{FertR} + NF_{FertVol}$; global consumption of inorganic N fertilizer (United Nations FAO, various years)
$PF_{Fert\ cons} = PF_{Fert\ crops} + PF_{Fert\ leach} + PF_{FertR} + PF_{Fert\ unr}$; global consumption of inorganic P fertilizer (United Nations FAO, various years)
$fN_{FertR} = 0.25$; fraction of applied N fertilizer that is lost in runoff (Smil, 1991)
$fN_{Fert\ crops} = 0.45$; fraction of applied N fertilizer that is assimilated into crops (Smil, 1991)
$fNP_{Fert\ leach} = 0.1$; fraction of applied N and P fertilizer that leaches into soilwater reservoir (Smil, 1991)
$fP_{FertR} = 0.1$; fraction of applied P fertilizer that is lost in runoff (Smil, 1991)

IID. Sewage Disposal

$CF_{Sewage} = fC_{Sewage} \times Pop_{global}(t)$; organic C from sewage discharges into coastal zone
$NF_{Sewage} = fN_{Sewage} \times Pop_{global}(t)$; total N from sewage discharges into coastal zone
$PF_{Sewage} = fP_{Sewage} \times Pop_{global}(t)$; total P from sewage discharges into coastal zone
$PF_{Detergent} = fP_{Detergent} \times Pop_{urban}(t)$; total inorganic P from detergent consumption
Pop_{global} = global population (United Nations Population Division, 1995)
Pop_{urban} = urban industrialized population (United Nations Population Division, 1995)
fC_{Sewage} = 1521 moles C/person/yr (Billen, 1993)
fN_{Sewage} = 261 moles N/person/yr (Billen, 1993)

fP_{Sewage} = 16.5 moles P/person/yr (Billen, 1993; Caraco, 1995)
$fP_{Detergent}$ = 30.6 moles P/urban industrial person/yr (Billen, 1993; Caraco, 1995)

III. CONSTANTS AND PARAMETERS

IIIA. Scaling factors in Terrestrial Photosynthetic Flux Equation

$K_{photo} = f_{C10} \times f_{Nsw} \times f_{Psw} \times f_T$
$f_{C10} = (R_{max,C}/CF_{101\ t=0}) \times [C_{10}(t)/(k_C + C_{10}(t))]$; atmospheric CO_2 response function, dimensionless
$R_{max,C} = 1.445 \times 10^5$ moles/yr
$k_C = 6.25 \times 10^5$ moles
$f_{Nsw} = (R_{max,N}/NF_{Sw1\ t=0}) \times [N_{Sw}(t)/(k_N + N_{Sw}(t))]$; soilwater N response function, dimensionless
$R_{max,N}$ = 566.9 moles/yr
k_N = 65.11 moles
$f_{Psw} = (R_{max,P}/PF_{Sw1\ t=0}) \times [P_{Sw}(t)/(k_P + P_{Sw}(t))]$; soilwater P response function, dimensionless
$R_{max,P}$ = 141.7 moles/yr
k_p = 2.04 moles
$f_T = Q_{10}^{\Delta T/10}$, temperature response function, dimensionless
Q_{10} = 2 (Ver, 1998)
$\Delta T = T(t) - T_{1700}$ global mean temperature change since the year 1700, in °C (UCAR/OIES, 1991; Houghton and others, 1996; Nicholls and others, 1996)

IIIB. Atmosphere–Ocean Exchange Flux

$(dC_4/dt)_{atmex} = [C_{4\ t=0}/[(R_0 \times C_{10\ t=0}) + [d \times (C_{10}(t) - C_{10\ t=0})]]] \times [1 - [d \times (C_{10}(t) - C_{10\ t=0})/[(R_0 \times C_{10\ t=0}) + [d \times (C_{10}(t) - C_{10\ t=0})]]]] \times dC_{10}/dt$
$(dC_7/dt)_{atmex} = [C_{7\ t=0}/[(R_0 \times C_{10\ t=0}) + [d \times (C_{10}(t) - C_{10\ t=0})]]] \times [1 - [d \times (C_{10}(t) - C_{10\ t=0})/[(R_0 \times C_{10\ t=0}) + [d \times (C_{10}(t) - C_{10\ t=0})]]]] \times dC_{10}/dt$
R_0 = 9; Revelle factor, dimensionless (Revelle and Munk, 1977)
d = 4; Revelle constant, dimensionless (Revelle and Munk, 1977)

IIIC. Surface Ocean–Deep Ocean Waters Exchange

$CF_{797} = -CF_{797\ t=0} + [(C_7(t) - C_{7\ t=0})/(h_7 \times \tau_9)] - [(C_9(t) - C_{9\ t=0})/(h_9 \times \tau_9)]$
h_9 = 3900 m; mean deep ocean water depth
h_7 = 100 m; mean surface ocean mixed layer depth
τ_9 = 500 yrs; time constant to disperse an ocean surface perturbation into the bulk oceans (Revelle and Munk, 1977)

IIID. Scaling factors in Marine Photosynthetic Flux Equation

$CF_{45} = CF_{45\ t=0} \times f_{N4} \times f_{P4}$
$CF_{78} = CF_{78\ t=0} \times f_{N7} \times f_{P7}$
$f_{N4} = N_4(t)/N_{4\ t=0}$
$f_{P4} = P_4(t)/P_{4\ t=0}$
$f_{N7} = N_7(t)/N_{7\ t=0}$
$f_{P7} = P_7(t)/P_{7\ t=0}$

IIIE. Redfield Ratios (additional Redfield Ratios given in text-section II)

$(C:N)_{1\ photo}$ = 10500/41.18
$(C:N)_{1\ resp}$ = 5250/41.18
$(C:N)_{2\ resp}$ = 2.05e4/976
$(C:N)_{5\ photo}$ = 600/90.71
$(C:N)_{8\ photo}$ = 3600/543
$(N:P)_{Crops}$ = 20
$(C:N:P)_{Sewage}$ = 32/5.5/1

$(C:P)_{1\ photo}$ = 10500/10.294
$(C:P)_{1\ resp}$ = 5250/10.294
$(C:P)_{2\ resp}$ = 2.05e4/147
$(C:P)_{5\ photo}$ = 600/5.66
$(C:P)_{8\ photo}$ = 3600/33.96

$(C:S)_{1\ photo}$ = 10500/8.235
$(C:S)_{1\ resp}$ = 5250/8.235
$(C:S)_{2\ resp}$ = 2.05e4/170.5
$(C:S)_{5\ photo}$ = 600/9.623
$(C:S)_{8\ photo}$ = 3600/57.736

References

Allen Jr., L. H., and Amthor, J. S., 1995, Plant physiological responses to elevated CO_2, temperature, air pollution, and UV-B radiation, *in* Woodwell, G. M., and Mackenzie, F. T., editors, Biotic Feedbacks in the Global Climatic System: Will the Warming Feed the Warming?: New York, Oxford University Press, p. 51–84.

Bacastow, R. D., and Keeling, C. D., 1973, Atmospheric carbon dioxide and radiocarbon in the natural carbon cycle: II. Changes from A.D. 1700 to 2070 as deduced from a geochemical model, *in* Woodwell, G. M., and Pecan, E. V., editors, Carbon and the Biosphere: Springfield, Virginia, U.S. Atomic Energy Commission, CONF-720510, p. 86–135.

Barnola, J. M., Anklin, M., Procheron, J., Reynaud, D., Schwander, J., and Stauffer, B., 1995, CO_2 evolution during the last millennium as recorded by Antarctic and Greenland ice: Tellus, v. 47B, p. 264–272.

Berner, E. A., and Berner, R. A., 1996, Global Environment: Water, Air and Geochemical Cycles: Upper Saddle River, New Jersey, Prentice Hall, 376 p.

Billen, G., 1993, The PHISON river system: A conceptual model of C, N and P transformations in the aquatic continuum from land to sea, *in* Wollast, R., Mackenzie, F. T., and Chou, L., editors, Interactions of C, N, P and S Biogeochemical Cycles and Global Change: Berlin, Springer-Verlag, p. 141–161.

Bischoff, W. D., Paterson, V. L., and Mackenzie, F. T., 1984, Geochemical mass balance for sulfur- and nitrogen-bearing acid components: Eastern United States, *in* Bricker, O. P., editor, Geological Aspects of Acid Deposition: Boston, Massachusetts, Butterworth Publishing, p. 1–21.

Bradley, R. S., Diaz, H. F., Eischeid, J. K., Jones, P. D., Kelly, P. M., and Goodess, C. M., 1987, Precipitation fluctuations over northern hemisphere land areas since the mid-19th century: Science, v. 237, p. 171–175.

Brady, N. C., and Weil, R. R., 1996, The Nature and Properties of Soils: Upper Saddle River, New Jersey, Prentice-Hall, Inc., 740 p.

Brown, L. R., Renner, M., and Flavin, C., 1997, The Environmental Trends that are Shaping Our Future: Vital Signs 1997: New York, W.W. Norton & Company, Inc., 165 p.

Bruno, M., and Joos, F., 1997, Terrestrial carbon storage during the past 200 years: a Monte Carlo analysis of CO_2 data from ice core and atmospheric measurements: Global Biogeochemical Cycles, v. 11, p. 111–124.

Cao, M., and Woodward, F. I., 1998a, Dynamic responses of terrestrial ecosystem carbon cycling to global climate change: Nature, v. 393, p. 249–252.

——— 1998b, Net primary and ecosystem production and carbon stocks of terrestrial ecosystems and their responses to climate change: Global Change Biology, v. 4, p. 185–198.

Caraco, N. F., 1995, Influence of human populations on P transfers to aquatic systems: A regional scale study using large rivers, *in* Tiessen, H., editor, Phosphorus in the Global Environment: Transfers, Cycles and Management. SCOPE 54: Chichester, England, John Wiley & Sons, Ltd., p. 235–244.

Ceulemans, R., and Mousseau, M., 1994, Effects of elevated atmospheric CO_2 on woody plants: The New Phytologist, v. 127, p. 425–426.

Charlson, R. J., Anderson, T. L., and McDuff, R. E., 1992, The sulfur cycle, *in* Butcher, S. S., Charlson, R. J., Orians, G. H., and Wolfe, G. V., editors, Global Biogeochemical Cycles: London, United Kingdom, Academic Press, p. 285–300.

Ciais, P., Tans, P. P., and Schimel, D. S., 1995, Partitioning of ocean and land uptake of CO_2 as inferred by $\delta\ ^{13}C$ measurements from the NOAA Climate Monitoring and Diagnostics Laboratory Global Air Sampling Network: Journal of Geophysical Research, v. 100, p. 5051–5070.

Ciais, P., Tans, P. P., Trolier, M., White, J. W. C., and Francey, R. J., 1995, A large northern hemisphere terrestrial CO_2 sink indicated by the $^{13}C/^{12}C$ ratio of atmospheric CO_2: Science, v. 269, p. 1098–1102.

Cole, J. J., Peierls, B. L., Caraco, N. F., and Pace, M. L., 1993, Nitrogen loading of rivers as a human-driven process, *in* McDonnell, M. J., and Pickett, S. T. A., editors, Humans as Components of Ecosystems: The Ecology of Subtle Human Effects and Populated Areas: New York, Springer-Verlag, p. 141–157.

Dai, A., Fung, I. Y., and Del Genio, A. D., 1997, Surface observed global land precipitation variations during 1900–88: Journal of Climate, v. 10, p. 2943–2962.

Deevey, E. S., 1973, Sulfur, nitrogen and carbon in the atmosphere, *in* Woodwell, G. M., and Peacan, E. V., editors, Carbon and the Biosphere: Springfield, Virginia, U.S. Atomic Energy Commission, CONF-720510, p. 182–190.

Delwiche, C. C., and Likens, G. E., 1977, Biological response to fossil fuel combustion products, *in* Stumm, W., editor, Global Chemical Cycles and Their Alterations by Man, Dahlem Konferenzen: Berlin, Germany, p. 73–88.

Diaz, H., Bradley, R. S., and Eischeid, J. K., 1989, Precipitation fluctuations over global land areas since late 1800s: Journal of Geophysical Research, v. 94, p. 1195–1210.

Dignon, J., 1992, NO_x and SO_x emissions from fossil fuels: a global distribution: Atmospheric Environment, v. 26, p. 1157–1163.

Dignon, J., and Hameed, S., 1989, Global emissions of nitrogen and sulfur oxides from 1860 to 1980: Journal Air Pollution Control Association, v. 39, p. 180–186.

Eamus, D., and Jarvis, P. G., 1989, The direct effects of increase in the global atmospheric CO_2 concentration on natural and commercial temperate trees and flowers: Advances in Ecological Research, v. 19, p. 1–55.

Esser, G., and Kohlmaier, G. H., 1991, Modeling terrestrial sources of nitrogen, phosphorus, sulphur and organic carbon to rivers, *in* Degens, E. T., Kempe, S., and Richey, J. E., editors, Biogeochemistry of Major World Rivers. SCOPE 42: Chichester, United Kingdom, John Wiley & Sons, p. 297–322.

Etheridge, D. M., Steele, L. P., Langenfelds, R. L., Francey, R. J., Barnola, J.-M., and Morgan, V. I., 1996, Natural and anthropogenic changes in atmospheric CO_2 over the last 1000 years from air in Antarctic ice and firn: Journal of Geophysical Research, v. 101, p. 4115–4128.

Friedli, H., Lotscher, H., Oeschger, H., Siegenthaler, U., and Stauffer, B., 1986, Ice core record of the $^{13}C/^{12}C$ ratio of atmospheric carbon dioxide in the past two centuries: Nature, v. 324, p. 237–238.

Friedlingstein, P., Fung, I., Holland, E., John, J., Brasseur, G., Erickson, D., and Schimel, D., 1995, On the contribution of CO_2 fertilization to the missing biospheric sink: Global Biogeochemical Cycles, v. 9, p. 541–556.
Galloway, J. N., Schlesinger, W. H., Levy II, H., Michaels, A., and Schnoor, J. L., 1995, Nitrogen fixation: Anthropogenic enhancement-environmental response: Global Biogeochemical Cycles, v. 9, p. 235–252.
Gates, D. M., 1985, Global biospheric response to increasing atmospheric carbon dioxide concentration, *in* Strain, B. R., and Cure, J. D., editors, Direct effects of increasing carbon dioxide on vegetation; Washington, District of Columbia, United States Department of Energy, ER-0238, p. 171–184.
Goudriaan, J., 1989, Modeling biospherical control of carbon fluxes between atmosphere, ocean and land in view of climatic change, *in* Berger, A., Schneider, S., and Duplessy, J. C., editors, Climate and Geo-Sciences: Kluwer Academic Publishers, p. 481–499.
Goudriaan, J., and Ketner, P., 1984, A simulation study of the global carbon cycle including man's impact on the biosphere: Climatic Change, v. 6, p. 167–192.
Grace, J., Lloyd, J., McIntyre, J., Miranda, A. C., Meir, P., Miranda, H. S., Nobre, C., Monroe, J., Massheder, J., Malhi, Y., Wright, I., and Gash, J., 1995, Carbon dioxide uptake by an undisturbed tropical rain forest in southwest Amazonia, 1992 to 1993: Science, v. 270, p. 778–780.
Hameed, S., and Dignon, J., 1992, Global emissions of nitrogen and sulfur oxides in fossil fuel combustion 1970–1986: Journal of the Air and Waste Management Association, v. 42, p. 159–163.
Harvey, L. D., 1989, Effect of model structure on the response of terrestrial biosphere models to CO_2 and temperature increases: Global Biogeochemical Cycles, v. 3, p. 137–153.
Houghton, J., Filho, L. G. M., Callander, B. A., Harris, N., Kattenberg, A., and Maskell, K., 1996, Climate Change 1995: The Science of Climate Change: Cambridge, United Kingdom, Cambridge University Press, 572 p.
Houghton, R. A., 1983, Changes in the carbon content of terrestrial biota and soils between 1860–1980: A net release of CO_2 to the atmosphere: Ecological Monographs, v. 53, p. 235–262.
——— 1991a, Release of carbon to the atmosphere from degradation of forests in tropical Asia: Canadian Journal of Forest Research, v. 21, p. 132–142.
——— 1991b, Tropical deforestation and atmospheric carbon dioxide: Climatic Change, v. 19, p. 99–118.
——— 1995, Effects of land-use change, surface temperature and CO_2 concentration on terrestrial stores of carbon, *in* Woodwell, G. M., and Mackenzie, F. T., editors, Biotic Feedbacks in the Global Climatic System: Will the Warming Feed the Warming?: Oxford, United Kingdom, Oxford University Press, p. 333–350.
Houghton, R. A., Davidson, E. A., and Woodwell, G. M., 1998, Missing sinks, feedbacks, and understanding the role of terrestrial ecosystems in the global carbon balance: Global Biogeochemical Cycles, v. 12, p. 25–34.
Hudson, R. J. M., Gherini, S. A., and Goldstein, R. A., 1994, Modeling the global carbon cycle: Nitrogen fertilization of the terrestrial biosphere and the "missing" CO_2 sink: Global Biogeochemical Cycles, v. 8, p. 307–333.
Idso, K. E., and Idso, S. B., 1994, Plant responses to atmospheric CO_2 enrichment in the face of environmental constraints: A review of the last 10 years' research: Agricultural and Forest Meteorology, v. 69, p. 153–203.
Ingall, E. D., and Van Cappellen, P., 1990, Relation between sedimentation rate and burial of organic phosphorus and organic carbon in marine sediments: Geochimica et Cosmochimica Acta, v. 54, p. 373–386.
Joos, F., and Bruno, M., 1998, Long-term variability of the terrestrial and oceanic carbon sinks and the budgets of the carbon isotopes ^{13}C and ^{14}C: Global Biogeochemical Cycles, v. 12, p. 277–295.
Kammen, D., and Marino, B., 1993, On the origin and magnitude of pre-industrial anthropogenic CO_2 and CH_4 emissions: Chemosphere, v. 26, p. 69–86.
Keeling, C. D., 1973a, The carbon dioxide cycle: Reservoir models to depict the exchange of atmospheric carbon dioxide with the oceans and land plants, *in* Rasool, S. I., editor, Chemistry of the Lower Atmosphere: New York, Plenum Press, p. 251–329.
——— 1973b, Industrial production of carbon dioxide from fossil fuels and limestone: Tellus, v. 25, p. 174–198.
Keeling, C. D., Chin, J. F. S., and Whorf, T. P., 1996, Increased activity of northern vegetation inferred from atmospheric CO_2 measurements: Nature, v. 382, p. 146–149.
Keeling, C. D., and Whorf, T. P., 1998, Atmospheric CO_2 records from sites in the SIO air sampling network, Mauna Loa Observatory, Hawaii, 1958–1997, Trends: A compendium of data on global change, http://cdiac.esd.ornl.gov/ftp/maunaloa-co2/maunaloa.co2: Oak Ridge, Tennessee, Oak Ridge National Laboratory, Carbon Dioxide Information Analysis Center.
Keeling, R. F., Piper, S. C., and Heimann, M., 1996, Global and hemispheric CO_2 sinks deduced from changes in atmospheric O_2 concentration: Nature, v. 381, p. 218–221.
Keeling, R. F., and Shertz, S. R., 1992, Seasonal and interannual variations in atmospheric oxygen and implications for the global carbon cycle: Nature, v. 358, p. 723–727.
Kindermann, J., Wurth, G., and Badeck, F.-W., 1996, Interannual variation of carbon exchange fluxes in terrestrial ecosystems: Global Biogeochemical Cycles, v. 10, p. 737–755.
Kohlmaier, G. H., Brol, H., Sire, E. O., Plochl, M., and Revele, R., 1987, Modeling estimates of plants and ecosystem response to present levels of excess CO_2: Tellus, v. 39B, p. 155–170.
Kohlmaier, G. H., Janecek, A., and Kindermann, J., 1990, Positive and negative feedback loops within the vegetation/soil system in response to a CO_2 greenhouse warming, *in* Bouwman, A. F., editor, Soils and the Greenhouse Effect: Chichester, United Kingdom, Wiley, p. 415–422.
Kolchugina, T. P., and Vinson, T. S., 1995, Role of Russian forests in the global carbon balance: Ambio, v. 24, p. 258–264.
Larcher, W., 1983, Physiological Plant Ecology (a translation of "Ökologie der Pflanzen" by M. A. Biederman-Thorson): Berlin, Germany, Springer-Verlag, 303 p.
Lashof, D. A., 1989, The dynamic greenhouse: Feedback processes that may influence future concentrations of atmospheric trace gases and climate change: Climatic Change, v. 14, p. 213–242.

Levy, H., Galloway, J. N., Eliassen, A., Fisher, B. E., Gorzelska, K., Hastie, D. R., Moody, J. L., Ryaboshapko, A. G., Savoie, D., and Whelpdale, D. M., 1990, The long-range transport of sulfur and nitrogen compounds, *in* Knap, A. H., editor, The Long-Range Atmospheric Transport of Natural and Contaminant Substances: Dordrecht, The Netherlands, Kluwer Academic Publishers, p. 231–257.

Likens, G. E., Bormann, H. F., and Johnson, N. M., 1981, Interactions between major biogeochemical cycles in terrestrial ecosystems, *in* Likens, G. E., editor, Some Perspectives of the Major Biogeochemical Cycles. SCOPE 17: New York, John Wiley and Sons, p. 93–112.

Likens, G. E., Mackenzie, F. T., Richey, J., Sedell, J. R., and Turekian, K. K., 1981, Flux of Organic Carbon by Rivers to the Oceans, Report 8009140: Washington, District of Columbia, United States Department of Energy, 397 p.

Logan, J. A., 1983, Nitrogen oxides in the troposphere: Global and regional budgets: Journal Of Geophysical Research, v. 88, p. 10785–10807.

Mackenzie, F. T., 1998, Our Changing Planet: An Introduction to Earth System Science and Global Environmental Change: Upper Saddle River, New Jersey, Prentice-Hall, Inc., 486 p.

Mackenzie, F. T., Lerman, A., and Ver, L. M., 1998, Role of the continental margin in the global carbon balance during the past three centuries: Geology, v. 26, p. 423–426.

Mackenzie, F. T., Ver, L. M., and Lerman, A., 1998, Coupled biogeochemical cycles of carbon, nitrogen, phosphorus, and sulfur in the land-ocean-atmosphere system, *in* Galloway, J. N., and Melillo, J. M., editors, Asian Change in the Context of Global Change: Cambridge, United Kingdom, Cambridge University Press, p. 42–100.

Mackenzie, F. T., Ver, L. M., Sabine, C., Lane, M., and Lerman, A., 1993, C, N, P, S global biogeochemical cycles and modeling of global change, *in* Wollast, R., Mackenzie, F. T., and Chou, L., editors, Interactions of C, N, P and S Biogeochemical Cycles and Global Change: Berlin, Germany, Springer-Verlag, p. 1–62.

Marland, G., Boden, T. A., Andres, R. J., Brenkert, A. L., and Johnston, C. A., 1998, Global, regional, and national CO_2 emissions, NDP-030/R8, Trends: A compendium of data on global change, http://cdiac.esd.ornl.gov/trends/emis/tre_glob.htm: Oak Ridge, Tennessee, Oak Ridge National Laboratory, Carbon Dioxide Information Analysis Center.

McGuire, A. D., Melillo, J. M., and Joyce, L. A., 1995, The role of nitrogen in the response of forest net primary production to elevated atmospheric carbon dioxide: Annual Review of Ecology and Systematics, v. 26, p. 473–503.

Melillo, J. M., Houghton, R. A., Kicklighter, D. W., and McGuire, A. D., 1996a, Tropical deforestation and the global carbon budget: Annual Reviews in Energy and Environment, v. 21, p. 293–310.

Melillo, J. M., McGuire, A. D., Kicklighter, D. W., Moore III, B., Vorosmarty, C. J., and Schloss, A. L., 1993, Global climate change and terrestrial net primary production: Nature, v. 363, p. 234–240.

Melillo, J. M., Prentice, I. C., Farquhar, G. D., Schulze, E. D., and Sala, O. E., 1996b, Terrestrial biotic responses to environmental change and feedbacks to climate, *in* Houghton, J., Filho, L. G. M., Callander, B. A., Harris, N., Kattenberg, A., and Maskell, K., editors, Climate Change 1995: The Science of Climate Change: Cambridge, United Kingdom, Cambridge University Press, p. 445–481.

Meybeck, M., 1982, Carbon, nitrogen, and phosphorus transport by world rivers: American Journal of Science, v. 282, p. 401–450.

Meyer, W. B., and Turner II, B. L., 1994, Changes in Land Use and Land Cover: A Global Perspective: Cambridge, United Kingdom, Cambridge University Press, 537 p.

Milliman, J. D., and Meade, R. H., 1983, Worldwide delivery of river sediment to the oceans: Journal of Geology, v. 91, p. 1–21.

Mousseau, M., and Saugier, B., 1992, The direct effects of increased CO_2 on gas exchange and growth of forest tree species: Journal of Experimental Botany, v. 43, p. 1121–1130.

Mulholland, P. J., and Elwood, J. W., 1982, The role of lake and reservoir sediments as sinks in the perturbed global carbon cycle: Tellus, v. 34, p. 490–499.

Myneni, R. B., Keeling, C. D., Tucker, C. J., Asrar, G., and Nemani, R. R., 1997, Increased plant growth in the northern high latitudes from 1981 to 1991: Nature, v. 386, p. 698–702.

Nadelhoffer, K. J., Emmett, B. A., Gundersen, P., Kjonaas, O. J., Koopmans, C. J., Schleppi, P., Tietema, A., and Wright, R. F., 1999, Nitrogen deposition makes a minor contribution to carbon sequestration in temperate forests: Nature, v. 398, p. 145–148.

Neftel, A., Moor, E., Oeschger, H., Turekian, K. K., and Dodge, R. E., 1985, Evidence from polar ice cores for the increase in atmospheric CO_2 in the past two centuries: Nature, v. 315, p. 45–47.

Nicholls, N., Gruza, G. V., Jouzel, J., Karl, T. R., Ogallo, L. A., and Parker, D. E., 1996, Observed climate variability and change, *in* Houghton, J., Filho, L. G. M., Callander, B. A., Harris, N., Kattenberg, A., and Maskell, K., editors, Climate Change 1995: The Science of Climate Change: Cambridge, United Kingdom, Cambridge University Press, p. 133–192.

Polglase, P. J., and Wang, Y. P., 1992, Potential CO_2 enhanced carbon storage by the terrestrial biosphere: Australian Journal of Botany, v. 40, p. 641–656.

Poorter, H., 1993, Interspecific variation in the growth response of plants to an elevated ambient CO_2 concentration: Vegetatio, v. 104/105, p. 77–97.

Quay, P. D., Tilbrook, B., and Wong, C. S., 1992, Oceanic uptake of fossil fuel CO_2: Carbon-13 evidence: Science, v. 256, p. 74–79.

Raich, J. W., Rastetter, E. B., Melillo, J. M., Kicklighter, D. W., Steudler, P. A., Peterson, B. J., Grace, A. L., Moore, B., and Vorosmarty, C. J., 1991, Potential net primary productivity in South America: Application of a global model: Ecological Applications, v. 1, p. 399–429.

Rao, J. L., and Berner, R. A., 1994, History of phosphorus in sediments of the Yangtze River (Chang Jiang) and its possible connection to the Yellow River (Huang He), AGU/ASLO Ocean Sciences Meeting: San Diego, California, American Geophysical Union, v. 75, p. 110.

Raynaud, D., and Barnola, J. M., 1985, An Antarctic ice core reveals atmospheric CO_2 variations over the past few centuries: Nature, v. 315, p. 309–311.

Redfield, A. C., Ketchum, B. H., and Richards, F. A., 1963, The influence of organisms on the composition of seawater, *in* Hill, M. N., editor, The Sea: New York, John Wiley and Sons, p. 26–77.
Revelle, R., and Munk, W., 1977, The carbon dioxide cycle and the biosphere, *in* Committee, N. G. S., editor, Energy and Climate: Washington, District of Columbia, National Academy Press, p. 140–158.
Sarmiento, J. L., Hughes, T. M. C., Stouffer, R. J., and Manabe, S., 1998, Simulated response of the ocean carbon cycle to anthropogenic climate warming: Nature, v. 393, p. 245–249.
Sarmiento, J. L., Orr, J. C., and Siegenthaler, U., 1992, A perturbation simulation of CO_2 uptake in an ocean general circulation model: Journal of Geophysical Research, v. 97, p. 3621–3645.
Schimel, D. S., 1995, Terrestrial ecosystems and the carbon cycle: Global Change Biology, v. 1, p. 77–91.
Schlesinger, W. H., 1997, Biogeochemistry: An Analysis of Global Change: San Diego, California, Academic Press, Inc., 588 p.
Sellers, P. J., Los, S., and Randall, D. A., 1996, A revised land surface parameterization (SiB2) for atmospheric GCMs. Part II: The generation of global fields of terrestrial biophysical parameters from satellite data: Journal of Climate, v. 9, p. 706–737.
Siegenthaler, U., Friedli, H., Loetscher, H., Moor, E., Neftel, A., Oeschger, H., and Stauffer, B., 1988, Stable-isotope ratios and concentration of CO_2 in air from polar ice cores: Annals of Glaciology, v. 10, p. 1–6.
Siegenthaler, U., and Sarmiento, J. L., 1993, Atmospheric carbon dioxide and the ocean: Nature, v. 365, p. 119–125.
Smil, V., 1985, Carbon, Nitrogen and Sulfur: Human Interference in Grand Biospheric Cycles: New York, Plenum Press, 459 p.
——— 1991, Population growth and nitrogen: An exploration of a critical existential link: Population and Development Review, v. 17, p. 569–601.
Smith, R. A., Alexander, R. B., and Wolman, M. G., 1987, Water-quality trends in the nation's rivers: Science, v. 235, p. 1607–1615.
Smith, S. V., and Hollibaugh, J. T., 1993, Coastal metabolism and the oceanic organic carbon balance: Reviews of Geophysics, v. 31, p. 75–89.
Smith, S. V., and Mackenzie, F. T., 1987, The ocean as a net heterotrophic system: Implications from the carbon biogeochemical cycle: Global Biogeochemical Cycles, v. 1, p. 187–198.
Tans, P. P., Berry, J. A., and Keeling, R. F., 1993, Oceanic $^{13}C/^{12}C$ observations: A new window on ocean CO_2 uptake: Global Biogeochemical Cycles, v. 7, p. 353–368.
Tans, P. P., Fung, I. Y., and Takahashi, T., 1990, Observational constraints on the global atmospheric CO_2 budget: Science, v. 247, p. 1431–1438.
Taylor, J. A., and Lloyd, J., 1992, Sources and sinks of CO_2: Australian Journal of Botany, v. 40, p. 407–420.
Tian, H., Melillo, J. M., Kicklighter, D. W., McGuire, A. D., Helfrich III, J. V. K., Moore III, B., and Vorosmarty, C. J., 1998, Effect of interannual climate variability on carbon storage in Amazonian ecosystems: Nature, v. 396, p. 664–667.
UCAR/OIES, 1991, Changes in Time in the Temperature of the Earth: Boulder, Colorado, UCAR/OIES.
United Nations FAO, 1995, Forest resources assessment 1990: Global synthesis: FAO Forestry Paper 124: Rome, Italy, Food and Agriculture Organization of the United Nations.
——— various years, Annual Fertilizer Review: Rome, Italy, Food and Agriculture Organization of the United Nations.
United Nations Population Division, 1995, World Population Prospects: The 1994 Revision: New York, United Nations, 884 p.
Ver, L. M., 1998, Global kinetic models of the coupled C, N, P, and S biogeochemical cycles: Implications for global environmental change, Ph.D. Dissertation Oceanography: Honolulu, University of Hawaii, 681 p.
Ver, L. M., Mackenzie, F. T., and Lerman, A., 1994, Modeling pre-industrial C-N-P-S biogeochemical cycling in the land-coastal margin system: Chemosphere, v. 29, p. 855–887.
——— 1999, Carbon cycle in the coastal zone: effects of global perturbations and change in the past three centuries: Chemical Geology v. 159, p. 283–304.
Wernick, I. K., Waggoner, P. E., and Ausubel, J. H., 1997, Searching for leverage to conserve forests: The industrial ecology of wood products in the United States: Journal of Industrial Ecology, v. 1, p. 125–145.
Wofsy, S. C., Goulden, M. L., Munger, J. W., Fan, S. M., Bakwin, P. S., Daube, B. C., Bassow, S. L., and Bazzaz, F. A., 1993, Net exchange of CO_2 in a mid-latitude forest: Science, v. 260, p. 1314–1317.
Wollast, R., and Mackenzie, F. T., 1989, Global biogeochemical cycles and climate, *in* Berger, A., Schneider, S., and Duplessy, J. C., editors, Climate and Geo-Sciences, Kluwer Academic Publishers, p. 453–473.
Woodwell, G. M., and Mackenzie, F. T., 1995, Biotic Feedbacks in the Global Climatic System: Will the Warming Feed the Warming?: New York, Oxford University Press, 416 p.
Woodwell, G. M., Mackenzie, F. T., Houghton, R. A., Apps, M., Gorham, E., and Davidson, E., 1998, Biotic feedbacks in the warming of the earth: Climatic Change, v. 40, p. 495–518.
Woodwell, G. M., Mackenzie, F. T., Houghton, R. A., Apps, M. J., Gorham, E., and Davidson, E. A., 1995, Will the warming speed the warming? *in* Woodwell, G. M., and Mackenzie, F. T., editors, Biotic Feedbacks in the Global Climatic System: Will the Warming Feed the Warming?: New York, Oxford University Press, p. 393–411.
Wullschleger, S. D., Post, W. M., and King, A. W., 1995, On the potential for a CO_2 fertilization effect in forests: Estimates of the biotic growth factor, based on 58 controlled-exposure studies, *in* Woodwell, G. M., and Mackenzie, F. T., editors, Biotic Feedbacks in the Global Climatic System: Will the Warming Feed the Warming?: New York, Oxford University Press, p. 85–107.